7-17-2017

The Brittle Deformation Sequence at Dead Indian Hill and the Heart Mountain Detachment, Wyoming, USA

G Graham Ellsworth

THE BRITTLE DEFORMATION SEQUENCE AT DEAD INDIAN HILL AND THE HEART MOUNTAIN DETACHMENT, WYOMING, USA

by

Guilford Graham Ellsworth

A Thesis
Submitted in Partial Fulfillment of the
Requirements for the Degree of
Master of Science

Major: Earth Sciences

The University of Memphis
August 2017

Dedication

To my Family

Acknowledgements

This thesis could not have been completed without the support from all the Faculty and Staff in Department of the Earth Sciences at the University - in particular; the guidance and teaching provided by Dr. Mervin J. Bartholomew. Working with him on this project has been a privilege and I owe much of my growth as a geologist to him. I thank him for introducing me to the Heart Mountain topic and all our discussions creating the foundation for this thesis.

Thank you to my committee members Dr. Randy Cox, Dr. Eunseo Choi; as well as, Earth Sciences faculty Dr. Daniel Larsen and Dr. Roy Van Arsdale, all of whom have been great teachers and resources and were always open to discuss any variety of geoscience topics, both linked and unconnected to this research.

This research was funded in part by the Colorado Scientific Society and the Tobacco Root Geological Society. Thank you to the kind folks at the Yellowstone Bighorn Research Association and the A.L. Michelson Field Station for their hospitality during my time in field. Cheers to my classmates at the University of Memphis and all the geologists along the way who provided amazing company and offered exciting insights into this research.

Lastly, thank you to those back home for the support, motivation and encouragement as I completed this thesis.

Abstract

Ellsworth, G. Graham. M.S. The University of Memphis. July 2017.
The Brittle Deformation Sequence of Dead Indian Hill and the Heart Mountain Detachment.
Major Professor: Dr. Mervin J. Bartholomew.

The Heart Mountain Detachment in northwestern Wyoming is one of the largest terrestrial mega-scale gravity-slides. The emplacement followed the Laramide Orogeny and contemporaneous with widespread Eocene activity in the Absaroka Volcanic Province. Analysis of fracture-sets (joints and faults) from selected outcrops of Cambrian to Eocene strata provide a stratigraphic framework for deciphering the regional sequence of brittle fractures. Seven fracture-sets elucidated from ~1,800 fracture azimuthal measurements, depict a brittle deformational sequence of the Pre-Eocene Laramide Orogeny, Absaroka Volcanism and the Heart Mountain Detachment. Three fracture-sets define a Pre-Eocene 48^{o} clockwise rotation of the stress-field associated with Pre-Laramide and Laramide tectonics. Four fracture-sets defined a 60^{o} counterclockwise rotation of the stress-field in the Eocene associated with Absaroka Volcanism, the Heart Mountain Detachment and the collapse of the volcanic edifice. Angular and abutting relationships of the pre-detachment fracture-sets identify the detachment rotated 30^{o} around a vertical axis as the volcanic system collapsed.

Table of Contents

List of Figures

INTRODUCTION

The Heart Mountain Detachment in Northwestern Wyoming is the best known and one of the largest gravity-slides mapped on Earth. Recent recognition of terrestrial mega-scale, gravity-slide structures adjacent to prominent ancient volcanic edifices challenges the limits distinguishing between gravitational and tectonic processes (Hacker et al., 2014; Biek et al., 2016). The classic Heart Mountain detachment is categorized as a rootless detachment with a steep dipping breakaway zone, which transitions downward into a low-angle basal decollement (Pierce, 1973; Anders et al., 2010). The detached mass - a thick rock package of ~1,100km^2 in area, had slid along the shallowly inclined surface (~2^o) across an aerial extent of ~3,400km^2 in the Eocene (~49ma) (Hauge, 1993; Malone et al., 2014). Parts of the detachment moved as much as 50km across the Wyoming landscape (Beutner and Gerbi, 2005). The detachment's extent and complex nature has challenged generations of geologists (Hewett, 1920; Bucher, 1947; Pierce 1973; Hauge, 1985; Beutner and Craven, 1996; Craddock et al., 2009; Anders et al., 2010; Malone et al., 2017), both before and after many major tectonic/structural breakthroughs occurred in balancing cross sections, plate tectonics, core complexes, and detachment faults.

The Heart Mountain detachment occurred during widespread Tertiary magmatism in the calc-alkali belt in the Rocky Mountains (Fig. 1). Within this belt, the Eocene Absaroka Volcanic Province (Malone, 2000) produced voluminous sequences of compositionally diverse rocks that, in the Eocene, covered previously exhumed Paleozoic and early Mesozoic sedimentary rocks (Fig. 2) (Sundell, 1993; Feeley and Cosa, 2003). The Mid-Paleozoic carbonate sequence (500m) and the Eocene volcanic cover (1000-3000m) make up the internal units of the detachment (Pierce, 1973; Beutner and Gerbi, 2005). Prominent basement-involved Pre-Laramide and Laramide structures, like the Beartooth Plateau (northern boundary) and Rattlesnake Mountain

(southeastern boundary), may constrain the detachment's lateral geometry inasmuch as to the west and south, most of the detachment is bordered by these uplifts (Fig. 3). Previous studies (e.g., Pierce, 1973; Hauge, 1985; Beutner and Craven, 1996; Malone, 2000; Craddock et al., 2009, Anders et al., 2010) suggested that the detachment ramped structurally upward over Dead Indian Hill and glided into the Bighorn Basin coming to rest where klippen (i.e. Heart Mountain and McCullough Peaks) remain (Hauge, 1993).

Here in, the sequence of fracture-sets (joints and faults) was determined from abutting, cross-cutting and angular relationships of brittle fractures from Cambrian through Eocene strata. Thus, structural relationships established within the stratigraphically continuous Paleozoic-Mesozoic section set the stage for distinguishing Pre-Laramide and Laramide fracture-sets from post-Laramide fracture-sets (i.e. Eocene) found in: 1) the Eocene Willwood Formation in the Bighorn Basin, 2) Eocene Absaroka dikes, 3) the White Mountain fault rocks, and 4) a small klippe of the Heart Mountain detachment.

Although the Heart Mountain Detachment has been rigorously studied, an explicit timeline of tectonic events and deformation at Dead Indian Hill has yet to be established. Assessing the kinematics of the brittle fractures within the detachment area permits construction of a timeline and assesses the origin of the anomalous western slope of Dead Indian Hill where part of the allochthon rests on Cambrian strata that is structurally below the detachment horizon in the Ordovician Bighorn Dolomite. Based on the relative timing of the slopes development from the fractures, it will be clear if the detachment ramped up the slope or the detachment surface was a continuous surface.

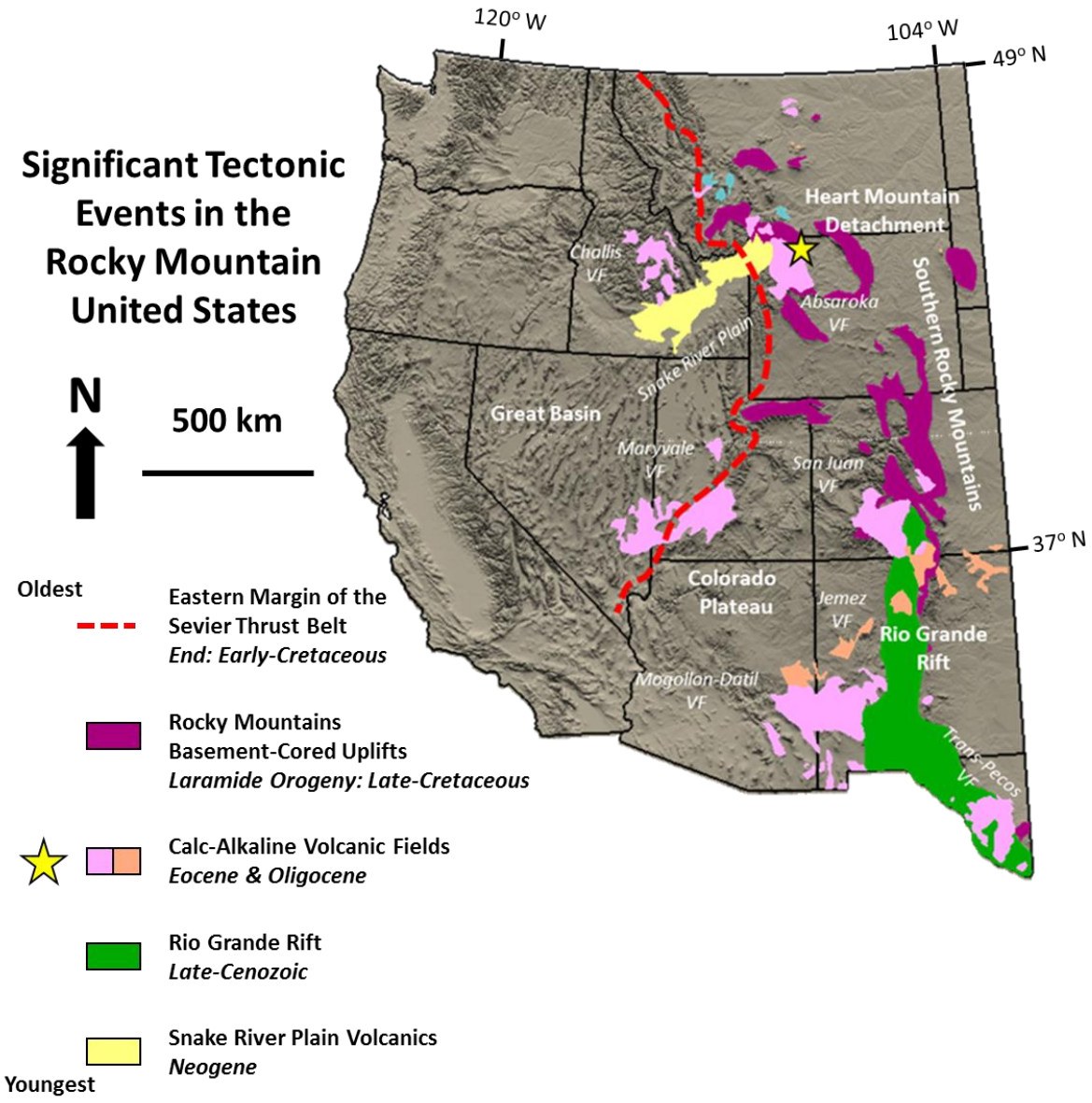

Figure 1: Tectonic Map of the Rocky Mountain Region

*M*ajor Mesozoic and Cenozoic tectonic features within the Rocky Mountain region. The eastern limit of the Sevier Thrust Belt (red dash line), prominent basement "pinned" Laramide uplifts (purple), the Rio Grande Rift (green), large Eocene-Oligocene volcanic provinces (Pink-Orange) and the relatively young Snake River Plain (Yellow). Location Heart Mountain detachment is the star on the northeast margin of the Absaroka Volcanic Field in northwest Wyoming.

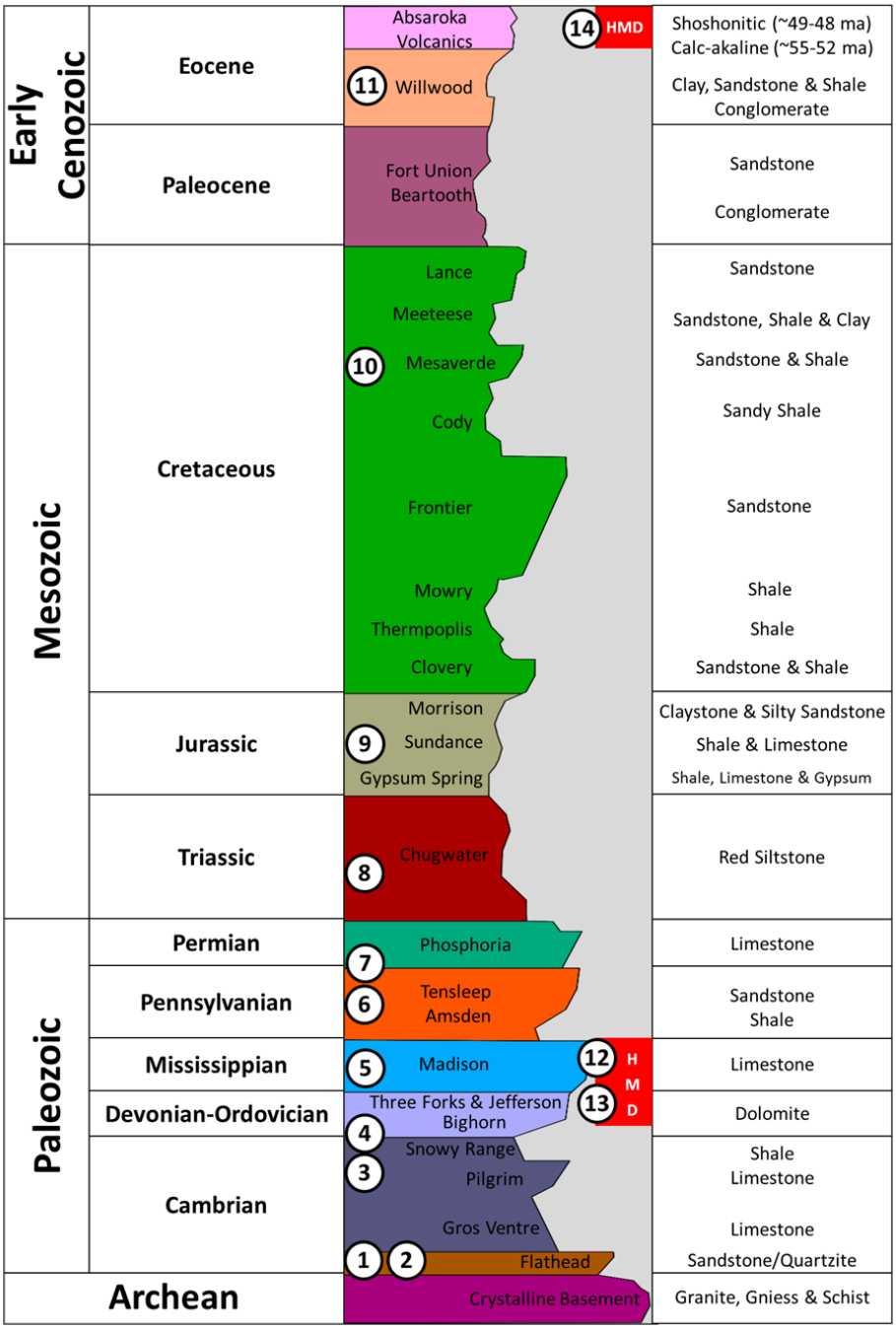

Figure 2: Representative stratigraphic column

Stratigraphy and unit descriptions of Dead Indian Hill following conventions of USGS geologic 7.5' quadrangles (Pierce, 1965a). Stratigraphic position of field locations where fracture data was collected are noted by the numbered circles. The Heart Mountain Detachment units are combined in the red boxes to the right. The basal detachment is in the lower section of the Bighorn Dolomite.

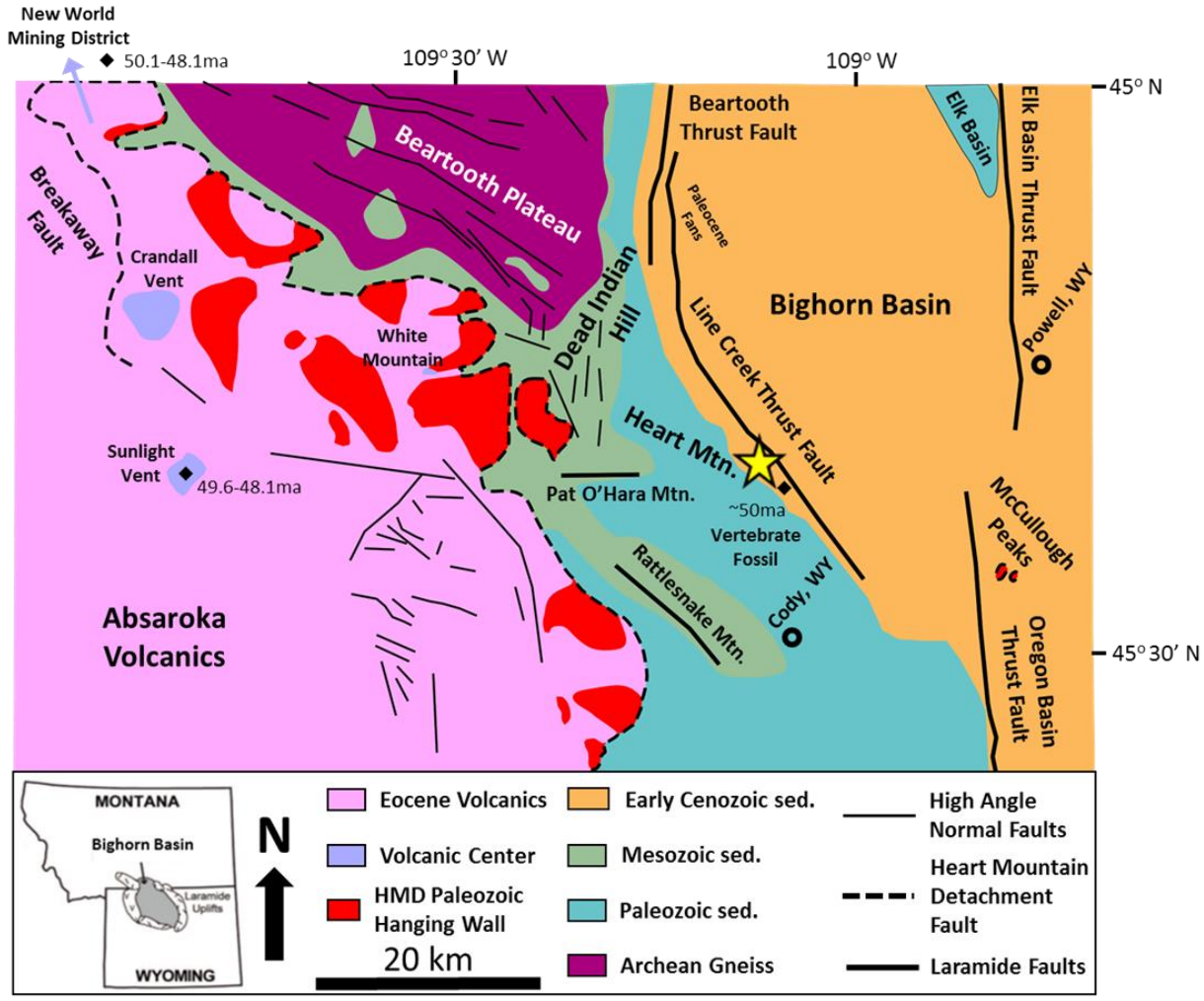

Figure 3: General geologic map of northwestern Wyoming

Modified from Erslev (1993) showing the prominent Laramide faults, Absaroka volcanic centers, margin of the Heart Mountain Detachment, the allochthonous klippe in the Bighorn Basin and young high-angle normal faults.

Station locations were primarily along an eastward-traverse adjacent to the Chief Joseph Highway (Hwy 296) starting from (Fig. 4):

1) Sunlight Creek, where the basal nonconformity of the Cambrian Flathead Formation is "pinned" to Archean basement (Location 1, Figure 4, EL. 1875m, Figure 5a), then
2) eastward and stratigraphically upward across Paleozoic strata and over Dead Indian Hill (where fresh road cuts expose highly fractured Tensleep Formation, EL. 2460m) (Locations 2-6, Figure 4, Figure 5b), then
3) eastward and stratigraphically upward across the Mesozoic strata ending in Cretaceous strata at the intersection with Wyoming Highway 120 (Locations 7-10, Figure 4, Figure 5c), then
4) farther east along hiking traverses in Eocene strata on the northern and southern perimeter of Heart Mountain (Location 11, Figure 4, Summit EL. 2430m, Fault Horizon EL. ~2100m, Figure 5d);
5) south of the Chief Joseph Highway along Sunlight Creek, from the classic exposure of the Heart Mountain detachment at White Mountain (Location 14, Figure 4, EL. 2100m, Figure 5e)
6) also along the Chief Joseph Highway on the western flank of Dead Indian Hill from well exposed strata within a klippe of the Heart Mountain detachment (Location 12-13, Figure 4 and Figure 5f).

Figure 4: Geologic map of Dead Indian Hill

After Pierce and Nelson (1968).. Numbered circles identify the localities along HWY 296 where fracture and data was collected.

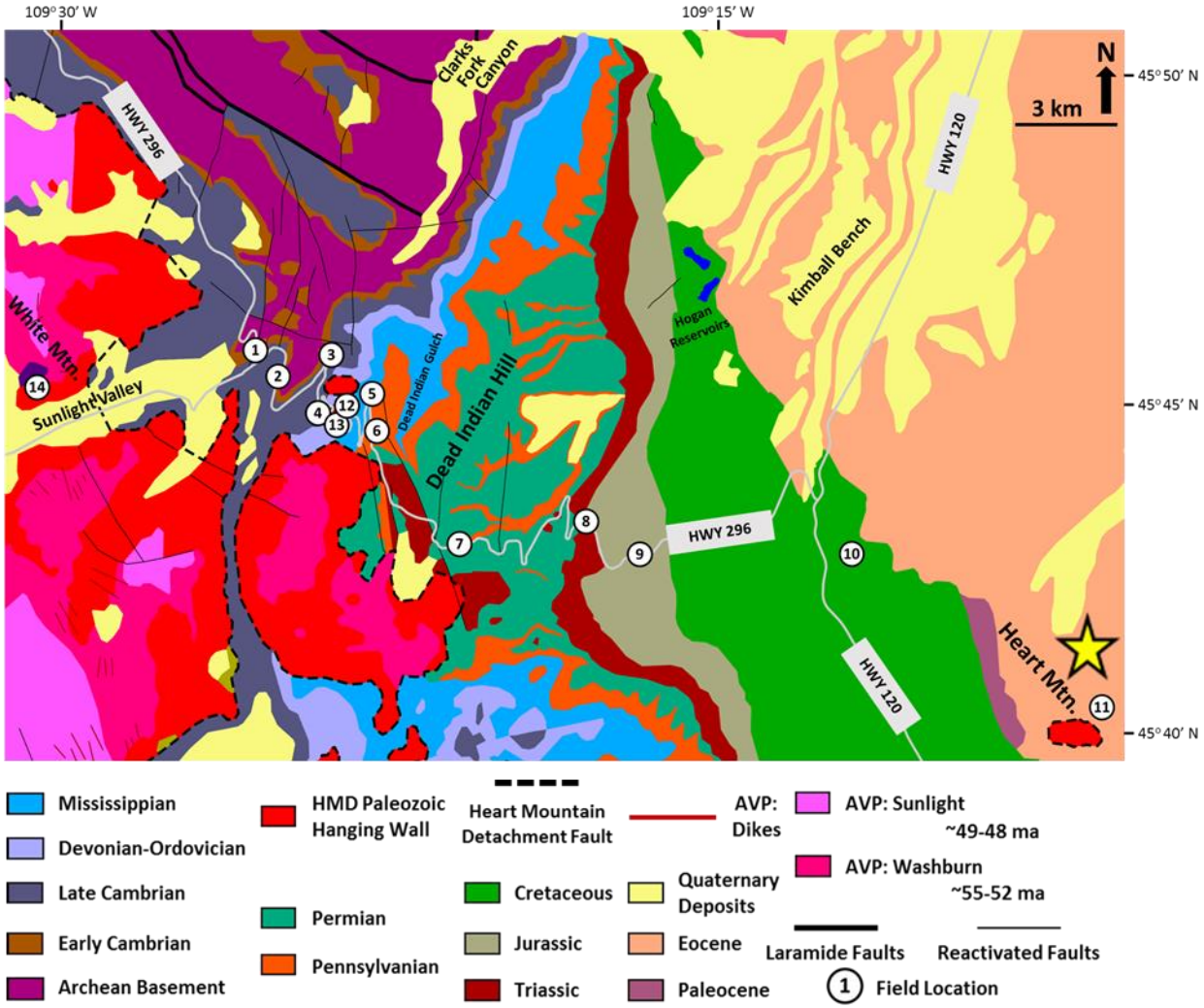

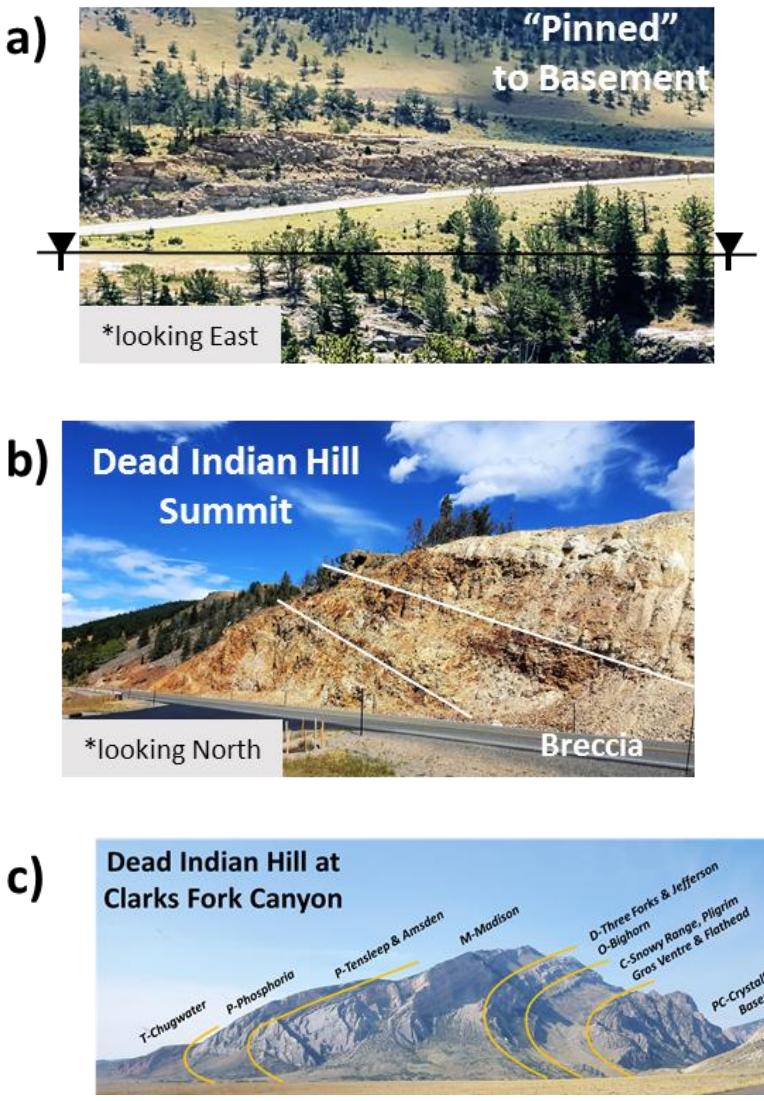

Figure 5: Critical Field Locations

5a) Sandstone of the Cambrian Flathead Formation "pinned" to the eroded Pre-Cambrian Granite surface in Sunlight Valley. Location 1 (EL. 1875m)

5b) Heavily fractured and brecciated sandstone of Tensleep Formation at the Dead Indian Hill Summit. Location 6 (EL. 2460m)

5c) Profile of the "pinned" to basement Dead Indian Hill strata folding eastward into the Bighorn Basin subsurface at the mouth of the Clarks Fork Canyon. (Summit EL. 2480m, Clark Fork River EL. 1335m)

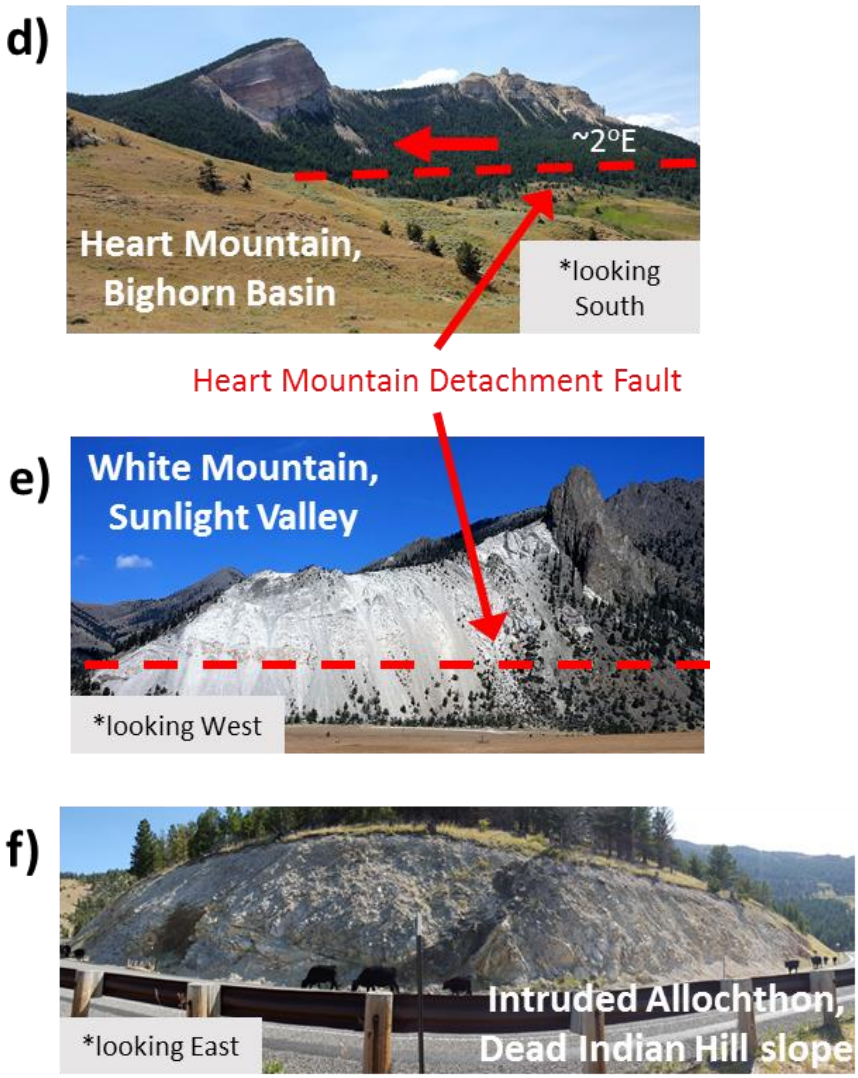

Figure 5: Critical Field Locations (continued)

5d) Heart Mountain in the Bighorn Basin, location 11 (Summit EL. 2430m). Red dashed line is the approximate east dipping contact of the detached Paleozoic carbonates and the Eocene sediment (contact EL. ~2100m).

5e) White Mountain in Sunlight Valley, location 14 (EL. 2100m). The intruded, marbleized, and detached Paleozoic section above the detachment fault which is exposed at the top of black layer on the southwest mountainside.

5f) Allochthon on the west slope of Dead Indian Hill, location 12. Absaroka Volcanism related dikes intrude the pre-existing fractures in the limestone of Madison Formation before the detachment event and subsequently transported by the detachment fault

GEOLOGICAL SETTING

Stratigraphy

Profiled in the steep cliffs at the mouth of the Clarks Fork River is a textbook profile of Paleozoic-Mesozoic sedimentary section "pinned" to the basement-cored Dead Indian Hill overturned anticline (Summit EL. 2480m, Clark Fork River EL. 1335m) (Fig. 5c). The stratigraphic terminology of this research follows the nomenclature of the published USGS quadrangles near Dead Indian Hill (Fig. 2) (Pierce, 1965a; Pierce, 1965b; Pierce and Nelson, 1968; 1971; Pierce et al., 1982). The Flathead Formation, through progressively younger strata to the Mesa Verde Formation are uniformly folded with the pinned granitic basement, and upper limb of the fold dips 40-60^{o} eastward into the Bighorn Basin (Blackstone, 1986). New road cuts along the Chief Joseph Highway (HWY 296) over Dead Indian Hill provide access to transported detachment-exposures of the Paleozoic Madison Limestone and Bighorn Dolomite.

East of Dead Indian Hill, basal strata of the Eocene Willwood Formation mark the E-dipping, Eocene-Cretaceous unconformity that crosses differentially eroded Cretaceous strata (Neser, 2014). At the Heart Mountain klippe, just below the detachment horizon, a biostratigraphic marker in the Eocene Willwood Formation provides an age of ~50Ma (Late-Wasatchian) (Gingerich, 1983) for when the Heart Mountain klippe was emplaced. From east to west, a trough of gently dipping sandstones frames the northern flank of the klippe.

At White Mountain, where the actual detachment fault horizon is exposed in the mountainside (Fig. 6a), the sub-detachment strata are mudstones of the Cambrian Snowy Range Formation and strongly metamorphosed Bighorn Dolomite. Here the detachment is in metamorphosed Madison Limestone and Bighorn Dolomite, which were intruded and altered by an Absaroka volcanic stock and dikes prior detachment (Beutner and Craven, 1996). The

detachment horizon is marked by a unique fault-rock layer of mixed volcanic-carbonate breccia; containing accreted, mantled, and rolled grains, along with non-fractured glass shards recognized as "Ultracatacaclastic Carbonate" (>80% carbonate matrix and <10% country rock clasts) (Craddock et al., 2009).

Absaroka Volcanism

Paleocene Laramide tectonic uplifts in northwestern Wyoming and Montana led to extensive erosion of Mesozoic and Paleozoic strata. Moreover, thermal expansion during widespread Absaroka Volcanism accompanied development of large stratovolcanoes where summits exceeded 3000m (Sundell, 1993) in the Absaroka Mountains west of Dead Indian Hill and Rattlesnake Mountain (Malone and Craddock, 2008). Absaroka magmas, erupted 55-45ma, are associated with an elevated Eocene crustal heat flux as a consequence of the detachment of lithospheric mantle of the subducted Farallon plate below North America and infiltration of asthenosphere above the foundering slab (Feeley, 2003).

The New World ($^{40}Ar/^{39}Ar$ age: 50.1-48.1ma) (Douglas et al., 2003), Crandall, and Sunlight vents ($^{40}Ar/^{39}Ar$ age: 49.6-48.1ma) (Feeley and Cosca, 2003) were prominent (Fig. 3) Eocene Absaroka volcanos associated with radial dike patterns and dike densities that are several times greater than depicted on geologic maps (Aharonov and Anders, 2006). Lavas, dikes and volcanoclastic deposits cap the exhumed Paleozoic units involved in the detachment (Malone, 2000). Dikes and vents intruded the regional Paleozoic carbonates prior to the detachment (DeFrates et al., 2006) (Fig. 6b), as noted at the classic White Mountain locality, where an ancillary volcanic stock intruded the Paleozoic formations (Fig. 6a); as well as, contributed to regional-scale hydrothermal fluid behavior of the detachment (Templeton et al., 1996; Douglas et al., 2003; Aharonov and Anders, 2006).

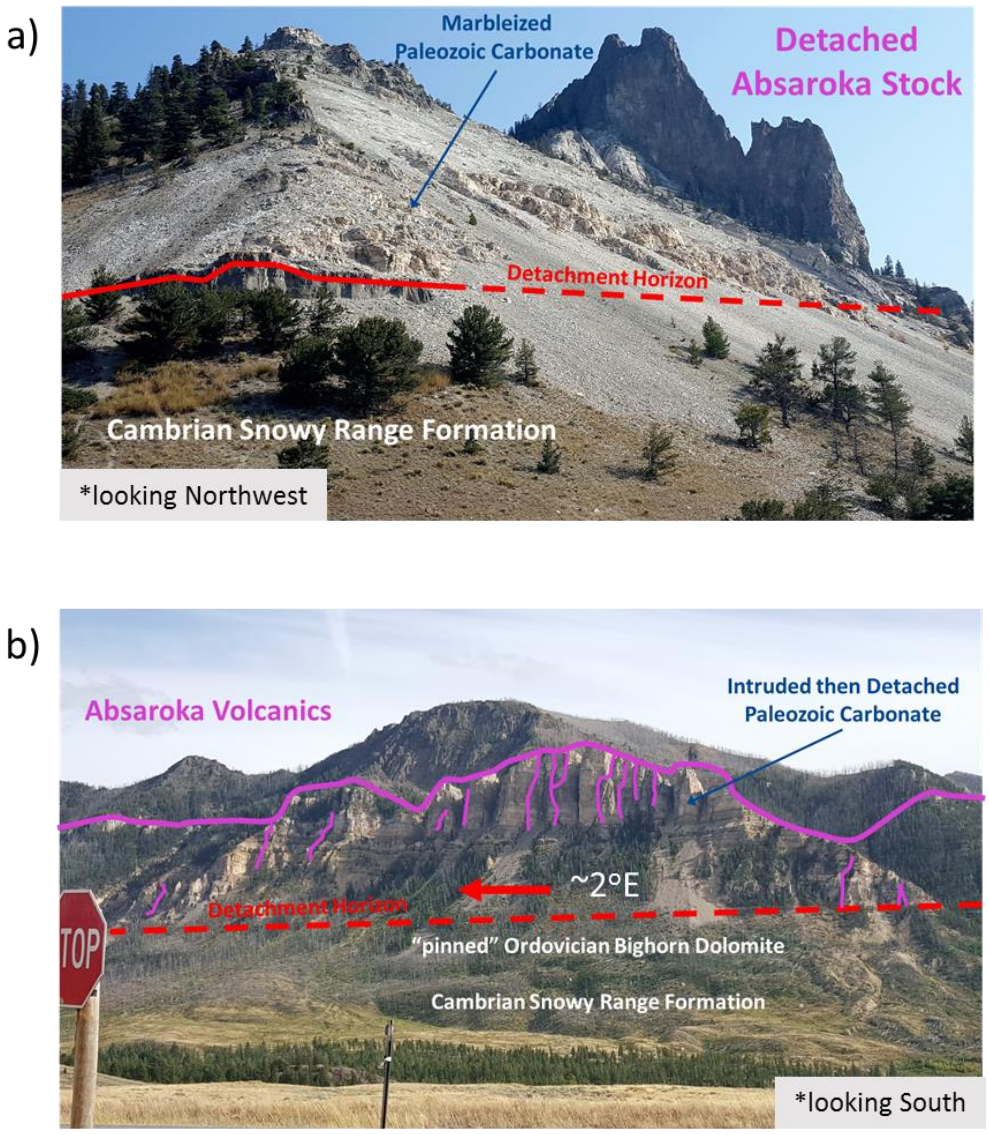

Figure 6: White Mountain and the detachment horizon

6a) The detachment horizon (Red line) exposed in the southwest slope immediately below the marbleized Madison and Bighorn formations. A pre-detachment volcanic stock intruded the Paleozoic carbonates and was subsequently truncated by the detachment fault.

6b) Absaroka dike intrusions in Paleozoic carbonate units in the "Bedding-Parallel" section, capped by Absaroka lavas, truncated and transported apart of the detachment event.

Basement-cored Laramide Uplifts

Preceding Eocene Absaroka volcanism and movement along the Heart Mountain detachment, much of western Wyoming had been deformed by large Cretaceous-Paleocene basement-cored ("thick-skinned") uplifts during the Laramide Orogeny. These uplifts extend away from the eastern flank of the E-vergent fold-thrust belt ("thin-skinned") of the Cretaceous Sevier Orogeny. In the United States, the eastern limit of the Sevier Orogen traces southward from the United States-Canada border across southwestern Montana, Idaho, the western most edge of Wyoming, and Utah (Fig. 1). The Sevier Orogeny initiated with Late-Jurassic subduction of the Farallon plate (DeCells, 2004). The Laramide Orogeny (75-35ma) in contrast, is principally defined by shallow-dipping (25^{o}-30^{o}) thrust faults originating in Precambrian crystalline basement-cored folds pinned to the nonconformable overlying sedimentary succession of Paleozoic and Mesozoic units (Fig. 5c) (Dickenson et al., 1988; Bird, 1998). The Laramide deformation locally in the Montana/Wyoming region produced NW-SE-trending uplifts (NE-SW-compression) (Gries, 1983) and established a significant relief between the uplifted crystalline blocks and the intermountain basins.

Near the Heart Mountain klippe, Laramide uplifts delineate the Bighorn Basin – a large isolated sedimentary basin, filled with eroded sedimentary cover from structurally uplifted and exhumed crystalline basement (DeCelles et al., 1991). The western margin of the basin is bound by the Beartooth Plateau, Dead Indian Hill, Pat O'Hara Mountain and Rattlesnake Mountain (Fig. 3).

The Beartooth Plateau, a topographically and structurally elevated block of Pre-Cambrian crystalline basement with over 3,000m of structural relief, reflects exhumation of Mesozoic and Paleozoic strata during NE-thrusting and development of syndepositional alluvial fans during the

Laramide Orogeny (Foose et al. 1961; Wise, 2000; DeCelles et al., 1991; Bartholomew et al., 2008; Stewart et al., 2008). These fans, found from the mouth of Clarks Fork Canyon (northward and eastward along the Beartooth front), demonstrate Paleocene to Early-Eocene unroofing of the Beartooth Plateau (DeCells et al., 1991), which was accompanied by large earthquakes (Bartholomew et al., 2008; Stewart et al., 2008). Campanian (Late-Cretaceous) paleoseismites (clastic dikes, convolute bedding) in the axial region of the Elk Basin anticline the Eagle Formation (Mesa Verde time equivalent) and younger units reflect the similar syntectonic deposition (Bartholomew et al., 2008; Jackson et al., 2016).

The Beartooth Plateau is separated from Dead Indian Hill by the deeply incised canyon of the Clarks Fork River (Fig. 4 and 5c). South of Dead Indian Hill lies E-W-trending Pat O'Hara Mountain and farther south is the iconic NW-trending Rattlesnake Mountain, a Laramide basement-cored fold (Erslev, 1993), which is asymmetrically folded with a steep W-dipping limb and a shallow E-dipping limb (Neely and Erslev, 2009; Beaudoin et al., 2012).

THE HEART MOUNTAIN DETACHMENT

Three competing models describe the behavior of the Heart Mountain detachment: 1) the Tectonic Denudation model of Pierce (1957, 1973, 1987); 2) the Continuous Allochthon model of Hauge (1985, 1990) and 3) the model for a catastrophic single detachment event (Beutner and Gerbi, 2005; Craddock et al., 2009, Anders et al., 2010). The models address three general structural themes for the detachment (Fig. 7a) (Pierce, 1973).

1) The 50km-long "bedding-parallel detachment," breaks steeply away at the surface for ~37km of lateral strike and traces down into a ~2^{o} dipping horizon parallel to a lower bedding plane of dolomite in the Bighorn Dolomite (Pierce, 1987). Most of the

detachment in this section lies near the primary Absaroka volcanic centers (Malone, 2000; Douglas et al., 2003).

2) The "transgressive-ramp" part crosses the western slope of Dead Indian Hill, where the detachment was interpreted to have moved upward across the Laramide fold. At Dead Indian Hill, the fault was interpreted to cut upward 5km at roughly a 10^{o} slope through Paleozoic and Mesozoic stratigraphy and across the fold crest (Pierce, 1973).
3) The third part constitutes erosional remnants (klippen) on top of Eocene strata in the Bighorn Basin as far as 45km east at Heart Mountain and McCullough Peaks (Pierce 1957). This third segment is referred to as the "Eocene-land-surface" segment, where early researchers observed the large klippen of coherent Bighorn and Madison Limestones are in fault contact with the underlying Willwood Formation (Eocene) (Hewett, 1920).

DETACHMENT MODELS

Tectonic Denudation model of Pierce

Pierce (1957) recognized the structure as a detachment feature and that tectonic denudation developed as pre-extrusive Absaroka earthquakes broke apart a continuous sheet of predominantly Ordovician, Devonian, and Mississippian strata. The detachment happened as a series of catastrophic transport-events which rapidly scattered detached remnants (via earthquake oscillation) across the landscape and exposed the fault surface between the allochthonous fragments (Pierce 1973). Following transport along the basal detachment, landslides, short-lived fluvial deposition, and voluminous Absaroka lavas then infilled and buried the fault surface and the allochthonous klippens (Pierce, 1987). Pierce's model shows the detachment having slid

southeastward, parallel to margin of the Beartooth uplift and crossing the Dead Indian Hill summit (Fig. 7b) (Pierce, 1957).

Continuous Allochthon Model of Hauge

Hauge interpreted the fault as a widespread detachment of a single sheet of Paleozoic rocks with a thick overburden of volcanic extrusive rocks (Hauge, 1990). Eruptions of Absaroka lavas (1-4km thick) coupled with contemporaneous faulting, initiated and perpetuated gravitational instability that caused non-catastrophic extension/thinning of the detachment sheet by normal, oblique-normal, and strike-slip faults in variable directions away from the volcanic centers and down-slope towards the Bighorn Basin (Fig. 7c) (Hauge, 1985). Hauge attributed significate extension to dike emplacement in the detachment sheet. The Continuous Allochthon model cites a "long-lived" detachment event. Cyclical periods of slip may have occurred along the fault due to temporary buildup of elastic loading via pressure-solution creep (Swanson et al., 2016).

Landslide Models

Petrographic and geochemical analysis of fault-rock at the detachment horizon at White Mountain suggest detachment occurred during a single event at a catastrophic rate due to intense volcanism (Fig. 7d) (Beutner and Gerbi, 2005., Craddock et al., 2009, Anders et al., 2010, Malone et al., 2017). The landslide models require trigger-mechanism for the slide, but need not be the same mechanism which sustained the slide. Increased volcanic activity at regional Absaroka volcanic centers led to the detachment, but the proposed "trigger" event could be: 1) a major eruption (Beutner and Gerbi, 2005); 2) failure of an inflated volcanic flank (Craddock et al., 2009) and/or 3) earthquakes associated with an increase of pore pressure due to dike injection (Aharonov and Anders, 2006). Models maintaining a singular long-runout of the detachment all

require drastic reduction of the coefficient of friction. Thermodynamic calculations suggest slip-duration was less than 4 minutes (slip-rates between 106-131 m/s) and that temperatures at the detachment horizon exceeded 600^{o} C during contact metamorphism of proximal carbonate rocks (Craddock et al., 2009). Thus, elevated temperatures facilitated thermal decomposition and generation of CO_2 gas along the slip zone (Mitchell et al., 2015). Goren et al. (2010) proposed that increased pore pressure, due to diking and frictional heating along the fault could produce rapid cycles of frictional heating and gas-fluidization resulting in transport of the slide mass via a basal fluidized medium (Anders et al., 2010). Calcite-twinning strain measured in the pinned Dead Indian Hill strata, indicates no detachment-related twinning strain or associated strain overprint (Craddock et al., 2000). Twining is time-dependent which requires with each overprint greater amounts of strain with each successive overprint. The absence of a twining overprint in the detachment area requires either a slip-rate at the basal horizon too great to induce calcite-twin deformation (Craddock et al., 2009), or the detachment never crossed Dead Indian Hill and the Bighorn Basin klippen originated from another location.

Figure 7: Detachment Models

7a) Illustrative profile of the Heart Mountain detachment fault geometry reproduced from Goren et al. (2010).

7b) Drawing of the two-phase Tectonic Denudation Model of Pierce (1973)*. 1) Earthquakes shattered a continuous sheet of Paleozoic carbonates 2) chaotic scatter individual blocks down the detachment slope and over Dead Indian Hill, creating aerial exposure of the detachment surface 3) infilled and cover of Absaroka lavas.

7c) Drawing of the prolonged Continuous Allochthon Model of Hauge (1985)*. A gravitational instability maintained by ongoing volcanism gradually dissected, thinned and extended a single a single sheet of Paleozoic carbonates and Absaroka lavas away from volcanic centers and down dip towards the Bighorn Basin.

7d) Generalized drawing of the Landslide Models (Beutner and Gerbi, 2005, Craddock et al., 2009, Anders et al., 2010)*. A singular detachment sheet catastrophically slid across the detachment region after an intense period of volcanism.

*Cross-sections drawings are from

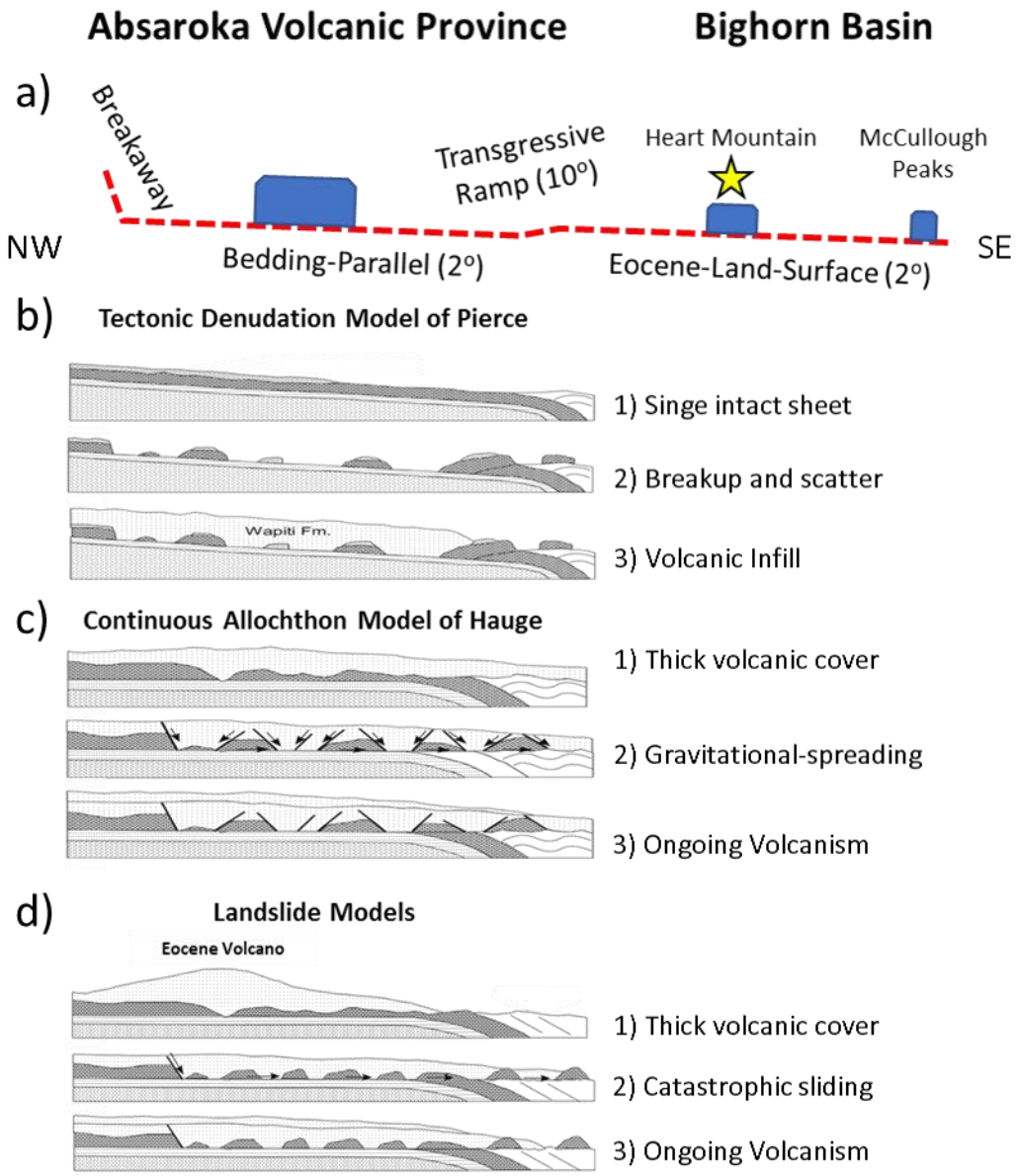

ANALYSIS METHODS

Because the Heart Mountain detachment is a rootless slide feature, older fracture orientations become passive markers of the pre-existing stress-fields. The angular offset of the fractures in the pinned stratigraphy and the fractures may reactivate during the slide but there will be an agreement of the kinematic indicators (slickenlines) indicating the azimuth which the slide was transported.

Relative ages of fracture-sets primarily were determined by using: 1) abutting relationships of joints; 2) crosscutting relationships of normal and reverse faults; and 3) when a joint, once formed in a fracture-set, could be reactivated as a normal, reverse, strike-slip or oblique-slip fault in a younger fracture-set. Here, joints are opening-mode brittle fractures that propagate at the fracture tip perpendicular to the least compressive stress direction (σ_3); whereas faults (either primary or reactivated) are associated with shearing modes of displacement (Fig. 8a) (Pollard and Aydin., 1988). Joints which abut into or curve off a pre-existing joint develop at a different time and under different stress conditions. These younger joints propagate as the stress field rotates through time (Bai and Gross, 1999). Where favorable, any misalignment of a pre-existing fracture to a younger stress field could cause a reactivation of the fracture in a shearing mode (Fig. 8b) (Wilkins et al., 2001). In this study, all dominant joint-sets typically display an orthogonal joint-set that likely reflect "stress-switching" indicative of a 90^o rotation of two principle stress orientations as joints form (e.g., minor fluctuation of horizontal stresses, local switching at the individual joint scale, or regional stress-switching of 90^o) (e.g., Dunne et al., 2003). Orthogonal joint-sets and reactivated orthogonal conjugate normal faults may form across near-surface regions of fold arches (Bartholomew and Whitaker, 2010).

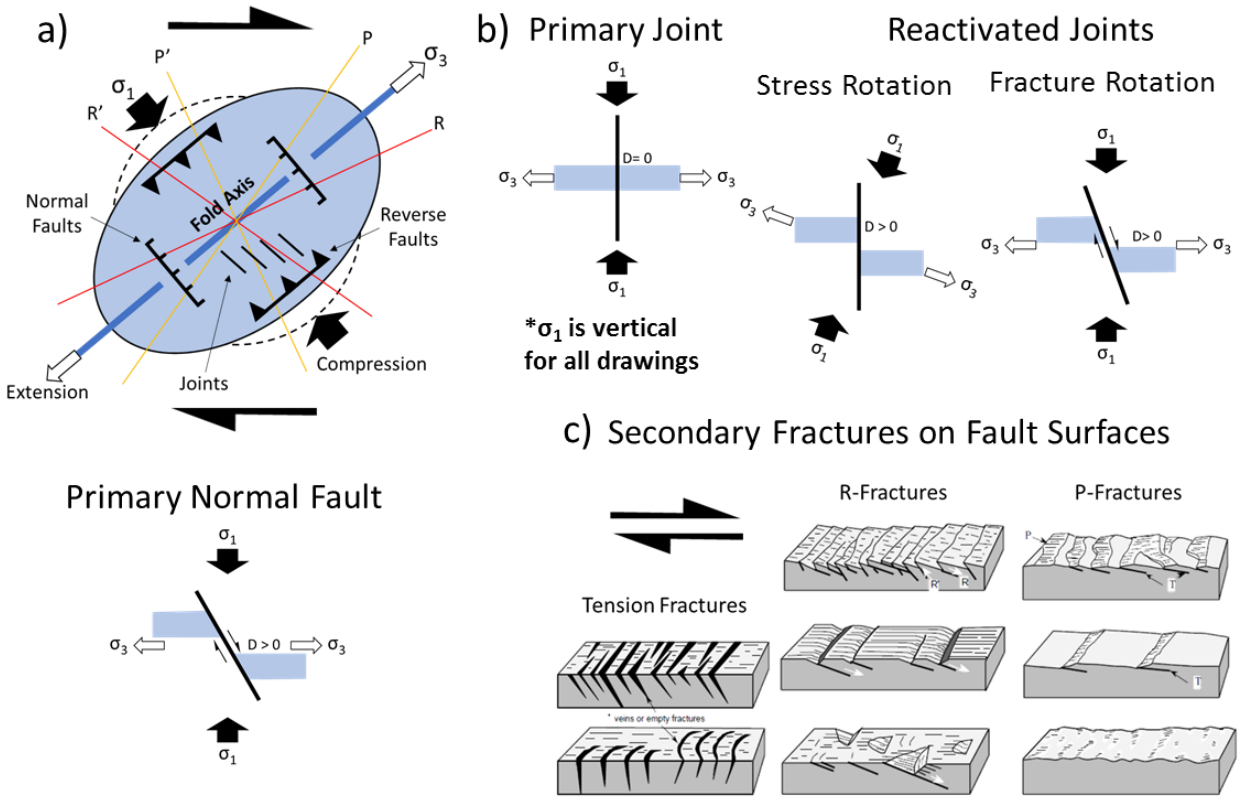

Figure 8: Brittle Fracture Kinematics

8a) Anticipated brittle fracture orientations.

8b) Fractures drawings modified from Wilkins et al. (2001) with σ_1 in a vertical position.

Joints: Opening-mode fractures which propagate in the direction of maximum horizontal stress and perpendicular to the least principle stress (σ3).

Faults: Fractures with visible shear displacement which propagate and slip in the same stress field.

Reactivations: Misalignment of the stress field to a fracture that causes shearing of a pre-existing fracture via a rotation of the stress field or rotation of the initial fracture.

8c) Petit (1987) criteria for assessing motion along a fault surface by means of secondary fractures. Block diagrams from Allmendinger et al. (1989).

DATA ANALYSIS

Collected data included bedding, joints, normal faults, reverse faults and strike-slip faults (Table 1). All orientation measurements followed the Right-Hand-Rule (RHR). Bedding strike and dip, measured at each field location, are used to restore folded strata and accompanying joints and faults to horizontal. For each recorded fracture, notes included the strike and dip, host rock, fracture type, fracture size and any abutting relationships. Along each fault-surface the pitch of each set of slickenlines was recorded along with notes on overprinting relationships and on the sense and amount of displacement and on any fault-surface features (Fig. 8c) (e.g., Petit, 1987).

Joints were first organized into sets (RHR) based similarity of strike, dip, and surface appearance, and then placed into a chronological sequence based upon all noted intersection relationships. Dip-slip and oblique-slip faults were combined into sets, along with overprinting and crosscutting relationships, based upon similarities of strike, dip, plunge azimuth of slickenlines, and sense of motion along each fault-surface. Correlation between the extension direction (σ_3) of conjugate normal faults and the opening direction (σ_3) of the dominate joint-sets, as well as relative ages of the joint-sets, identified the primary dip-slip faults from fractures which had been subsequently reactivated as younger oblique-slip faults (Bartholomew and Whitaker, 2010). Reverse faults were correlated with fracture-sets based on agreement of the azimuth of slickenlines vectors (σ_1) which were aligned with the strike of the dominant joint planes (σ_1 or H_{Max}; $+/-10^o$-15^o).

Table 1: Fracture Table

Fracture types that make up the Pre-Eocene and Eocene fracture sequences. The Heart Mountain Detachment occurred in the Eocene after the end of the Laramide orogeny and following beginning of Absaroka Volcanism

	Types of Fractures and Faults				Fracture Set	Mean Strike	Abutting Relationships	Fracture Reactivations	Opening/Extension Direction (σ_3 or h_{min})	Compression Direction (σ_1 or H_{max})
Event	Joints	Normal	Reverse	Strike-Slip						
PL1	390	5			L1	002°-182° ± 15°	41	0	092°-272°	002°-182°
					$L1_o$	092°-272° ± 15°	17			
L1	323	22	2		L2	027°-207° ± 10°	38	8	117°-297°	027°-207°
					$L2_o$	117°-297° ± 10°	21			
L2	171	36	5		L3	050°-230° ± 10°	9	33	140°-230°	050°-230°
					$L3_o$	140°-320° ± 10°	10			
E1	359	57	4		E1	157°-337° ± 10°	46	41	067°-247°	157°-337°
					$E1_o$	067°-247° ± 10°	38			
E2		17		LL: 37 RL: 24	E2a E2b	No Joints	0	78	130°-310°	158°-338°
E3	33	9			E3	128°-308° ± 10°	5	9	038°-218°	128°-308°
					$E3_o$	038°-218° ± 10°	1			
E4	181	39			E4	097°-277° ± 10°	16	39	007°-187°	097°-277°
					$E4_o$	007°-187° ± 10°	13			
Total	1457	185	11	61	**Overall: 1714**		255	208	Total Number of Age Relationships: 463	

Paleozoic | Paleozoic & Mesozoic | Paleozoic, Mesozoic & Eocene | Absaroka Volcanics | Heart Mountain Detachment

A total of 1783 bedding, joint and fault measurements were collected at 14 localities in Cambrian-Eocene sedimentary, igneous, and metamorphic rocks in the pinned strata and within the allochthonous klippen of the detachment-block (Table 1, Figure 4). In all, 27% or 463/1714 of joints collected in this study displayed age-relationships. The consistent time and angular arrangement of abutting joints coupled with gross population counts for each joint-set, was used to determine which fracture-sets are related to either Pre-Laramide, Laramide events or post-Laramide Eocene events. Data was either plotted on equal-area, lower-hemisphere stereographic projections or as rose diagrams (azimuth, 0^o-360^oRHR) to portray spatial representation, age relationships and overall number count of structural features.

Pre-Eocene Fractures Below the Detachment

Bedding and fracture data (joints and meso-faults) collected in the Flathead Formation through the Mesa Verde Formation on the Dead Indian Hill fold elucidates three fracture events (Fig. 9 & Figure 10). The pinned Dead Indian Hill fracture dataset (as a whole) includes: 141 of 864 or 16% of joint orientations which display age relationships, 12 dip/slip normal and reverse faults; as well as, 69 observed joints or dip/slip faults which were reactivated in oblique-normal or oblique-reverse sense of slip.

The PL1 fracture-set is the oldest, occurs throughout the Paleozoic stratigraphy, and is a significant population of near vertical joints which primarily strike 002^o-$182^o \pm 15^o$. $PL1_o$ is a minor orthogonal joint-set that strikes 092^o-$272^o \pm 15^o$ (Table 1; Figure 10). Younger joint-sets abut into PL1 fracture surfaces and PL1 joints are commonly reactivated in later events. PL1 was not observed in Mesozoic and younger strata. PL1 preceded or was coeval (via "stress-switching") with the $PL1_o$. The orthogonal relationship likely resulted from local stress-switching (by any mechanism) during PL1 joint formation (Dunne et al., 2003).

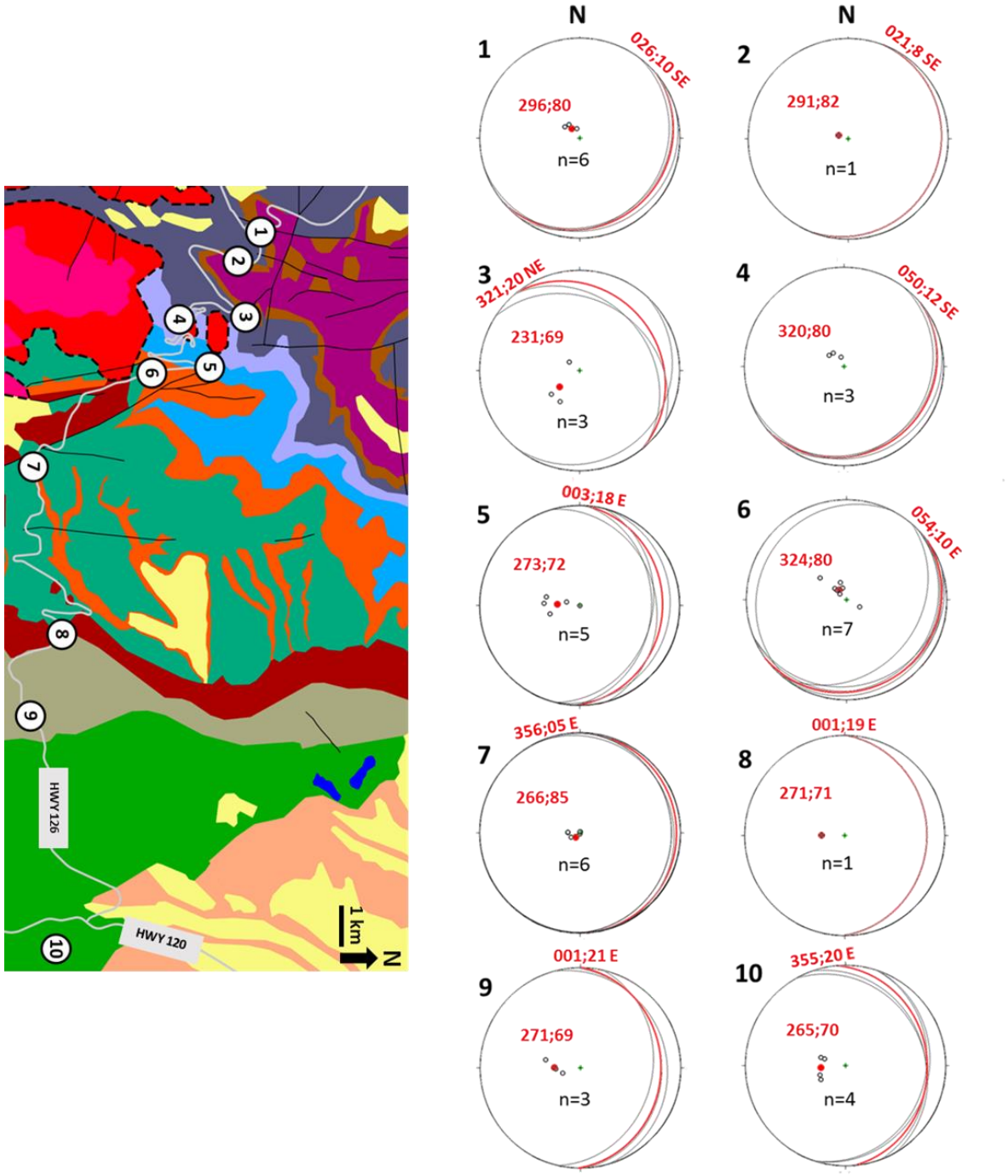

Figure 9: "Pinned" Dead Indian Hill Bedding

Stereographic projections demonstrating the predominantly west to east steepening of the "pinned" bedding along the Dead Indian Hill anticline limb. Bedding planes are in black, the poles-to-bedding planes are hollow dots. The red planes and red dots are the mean orientation of the bedding at each field station

A single PL1 dip-slip normal fault was measured below the detachment horizon. Joints of PL1 are the largest and most through going fracture faces in outcrop. PL1 and $PL1_o$ surfaces averaged $1.5m^2$ in surface-area. In the almost flat lying Flathead Formation, nonconformably pinned to the eroded basement surface, a significant number of joints of measured (102/212) at this location are part of the PL1 joint-set (Fig. 10). Although older fracture sets exist in Precambrian granitic rocks beneath the Flathead, they were not evaluated in this study.

The L1 fracture-set contains joints, normal faults and reverse faults that all mark the beginning of the Laramide Orogeny in northwestern Wyoming. L1 joints strike 027^o-$207^o \pm 10^o$ with a minor $L1_o$ joint-set that strikes 117^o-$297^o \pm 10^o$ (Table 1; Figure 10). Normal faults occur as both dip-slip faults and reactivations of pre-existing PL1 fractures. Slip-vectors of reverse faults match the orientation of L1 joints. The L1 fracture-set, oldest in Mesozoic strata, is younger in Paleozoic strata, and tend to curve away from PL1 fractures.

The L2 fracture-set is differentiated by joints, reverse faults, joint-reactivations as normal faults and reactivated L1 reverse faults. Joints of L2 strike 050^o-$230^o \pm 10^o$ and $L2_o$ strikes 140^o-$230^o \pm 10^o$ (Table 1; Figure 10). Normal faults occur as joint-reactivations of PL1 and L1 fractures. Reverse faults are dip-slip and reactivations of L1 reverse fault planes. Reverse fault slip-vectors complement the orientation L2 joints.

Pre-Eocene Fractures in the Allochthon
(small klippe on western flank of Dead Indian Hill; herein referred to as "the allochthon")

After restoration of the allochthon's bedding to horizontal (Fig. 11a,b), the same Pre-Eocene fracture-framework of joint populations and age relationships are evident in the allochthon as was established for Pre-Laramide and Laramide fractures pinned to basement below the detachment horizon.

Figure 10: Dead Indian Hill Pre-Eocene Sequence

The Pre-Eocene Fractures in the "pinned" strata at Dead Indian Hill. The rows indicate the relative timing sequence of Laramide fracture events. The columns to the right indicate with the stereographic projections the mode of deformation of the fractures. The maps to the left shows the distribution of joints at each field station. Rose diagrams in the maps are normalized to 10 rose pedals equals 100%.

Hollow arrows
opening/extension direction

Black arrows
compression direction
Interior Ratio
total # joints/# joint ages (i.e. abutting relationships)

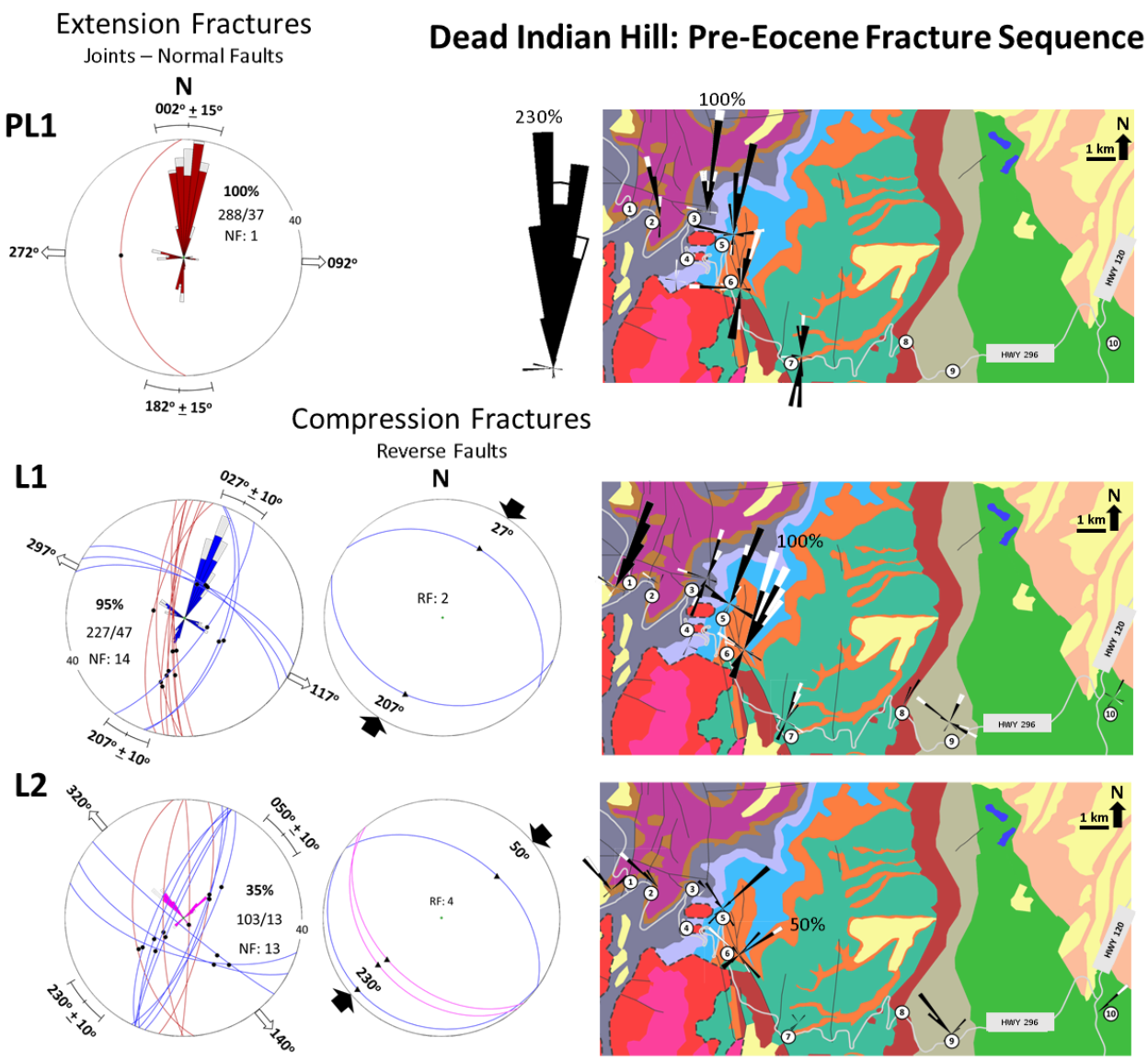

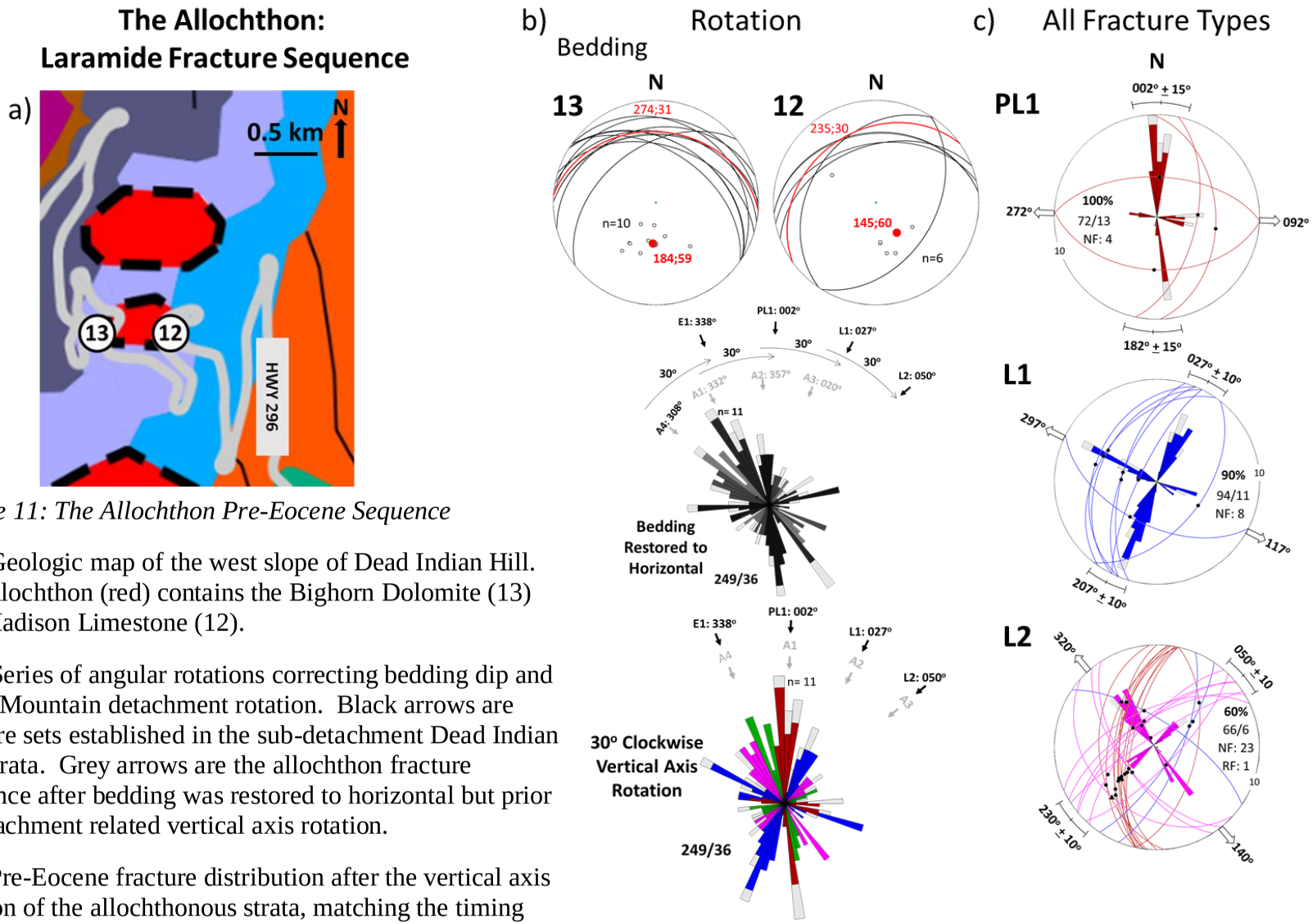

Figure 11: The Allochthon Pre-Eocene Sequence

11a) Geologic map of the west slope of Dead Indian Hill. The allochthon (red) contains the Bighorn Dolomite (13) and Madison Limestone (12).

11b) Series of angular rotations correcting bedding dip and Heart Mountain detachment rotation. Black arrows are fracture sets established in the sub-detachment Dead Indian Hill strata. Grey arrows are the allochthon fracture sequence after bedding was restored to horizontal but prior to detachment related vertical axis rotation.

11c) Pre-Eocene fracture distribution after the vertical axis rotation of the allochthonous strata, matching the timing sequence of fracture and the bulk population found in the Paleozoic strata "pinned" beneath the allochthon, which confirms the Laramide sequence.

Furthermore, the similarity of joint-orientation and the relative fracture-sequence was used to determine how much rotation about a vertical axis occurred after the detachment slid relative to the pinned counterparts (Fig. 11b). The Paleozoic units in the allochthon's road-cut need a clockwise rotation in the Madison Limestone of 30^{o} and the Bighorn Dolomite 27^{o} to match the three bulk joint trends in pinned Dead Indian Hill strata (Fig. 10 & Figure 11 b,c). This means the Pre-Laramide and Laramide joints rotated counterclockwise ~30^{o} while sliding.

The orthogonal joint-set of PL1 (002^{o}-182^{o}/092^{o}-272^{o} $\pm$ 15^{o}) and normal faults appear in both the Madison Limestone and in the Bighorn Dolomite. Intersecting PL1 joints, L1 (027^{o}-207^{o}/117^{o}-297^{o} $\pm$ 10^{o}), L2 (050^{o}-230^{o}/140^{o}-230^{o} $\pm$ 10^{o}) and E1 (introduced in the text following this section) joint development occurred in the same sequence and with the same angular arrangement as in the pinned strata (Fig. 10 & Figure 11c). Both Laramide sets have both dip-slip and oblique reactivations of preceding fracture-sets.

White Mountain Fractures

At the well-studied White Mountain locality, several meters below the detachment horizon, exposed nearly horizontal Snowy Range Formation has a joint sequence that is the same as the pinned section in flat lying Flathead Formation across the Sunlight Valley at Dead Indian Hill (Fig. 4). No bedding, fault, or fold-related rotations were necessary to identify the sequence and angular arrangement of PL1, L1 or L2 fracture sets (Fig. 12a).

However, immediately below the detachment, altered Bighorn Dolomite and fault breccia (carbonate ultracataclaycite of Craddock et al., 2009) (Fig. 12b,c) contain abutting joint relationships which elucidate three of four Eocene fracture events. The first Eocene fracture-set (E1) trends 157^{o}-337^{o} $\pm$ 10^{o} and is associated with an orthogonal fracture-set (E1$_{o}$) that trends 067^{o}-247^{o} $\pm$ 10^{o}. Because of an ~60^{o} cutoff angle relative to bedding, E1 is a series of inferred

dip-slip normal faults (Fig. 12c). These faults lack mesoscopic indicators of slip (slickenlines, displacement, secondary fractures, etc. …).

The E2 fracture-set is a collection of strike-slip faults within the allochthon along the western slope of Dead Indian Hill and were not observed at White Mountain. The E3 fracture-set and its orthogonal pair ($E3_o$) (128^o-308^o/038^o-$218^o \pm 10^o$) abut E1 joints. The youngest fracture-set (E4) consists of joints that strike 097^o-$277^o \pm 10^o$ and oriented 007^o-$187^o \pm 10^o$. Both E3 and E4 joints abut into the E1 fractures.

Eocene Fractures in the Willwood Formation

The Pre-Laramide and Laramide fracture-sets were not recognized in any Eocene strata; therefore, all fracture-sets in the Willwood Formation postdate Laramide deformation. Again, three of the four Eocene joint-sets were observed along hiking traverses in the Willwood Formation leading to the northern flank of Heart Mountain (Fig. 13a). These three joint-sets are similar to those at White Mountain, after corrections for bedding dip. The two older Eocene joint-sets trend NW and the youngest orthogonal joint-pair trends N-S/E-W. Bedding in the Willwood Formation both near and west of Heart Mountain (Neser, 2014), define a small fold with a trough axis that trends 312^o adjacent to the Heart Mountain klippe (Fig. 13b).

E1-joints trend 157^o-$337^o \pm 10^o$ and minor $E1_o$-joints trend 067^o-$247^o \pm 10^o$. Like at White Mountain, no strike-slip faults related to E2 were observed in the Willwood Formation. E3-joints trend 128^o-$308^o \pm 10^o$ and minor $E3_o$-joints trend 038^o-$218^o \pm 10^o$ (Table 1 & Figure 13c). The youngest Eocene joint-set (E4 and $E4_o$) is 097^o-$277^o \pm 10^o$ and 007^o-$187^o \pm 10^o$ respectively (Fig. 13c).

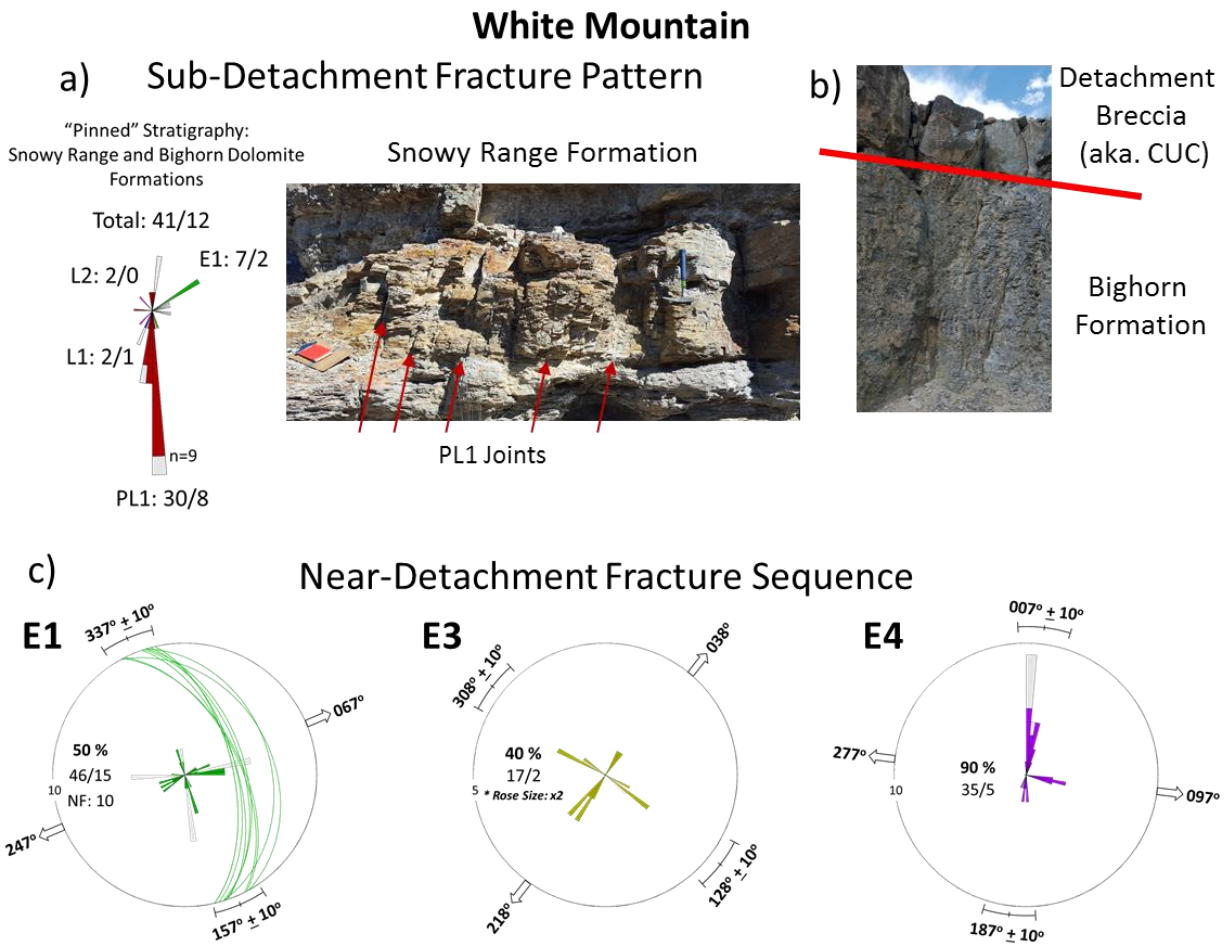

Figure 12: White Mountain Pre-Eocene and Eocene Sequences

12a) Rose diagrams and image of PL1-joints in the horizontal Snowy Range and Bighorn formations below the detachment.

12b) The detachment horizon (red line) at White Mountain. Carbonate Ultracataclasite fault rock (CUC) above altered dolomite of the Bighorn.

12c) Stratigraphic projections of Eocene fracture-sets in the CUC horizon and the altered Bighorn Formation dolomite immediately below the detachment. The faults of E1 are inferred dip-slip normal faults. Rose pedals normalized to a maximum perimeter of 5 is 100%.

*Note the E3 rose diagram perimeter is half the diameter of E1 and E4 diagrams.

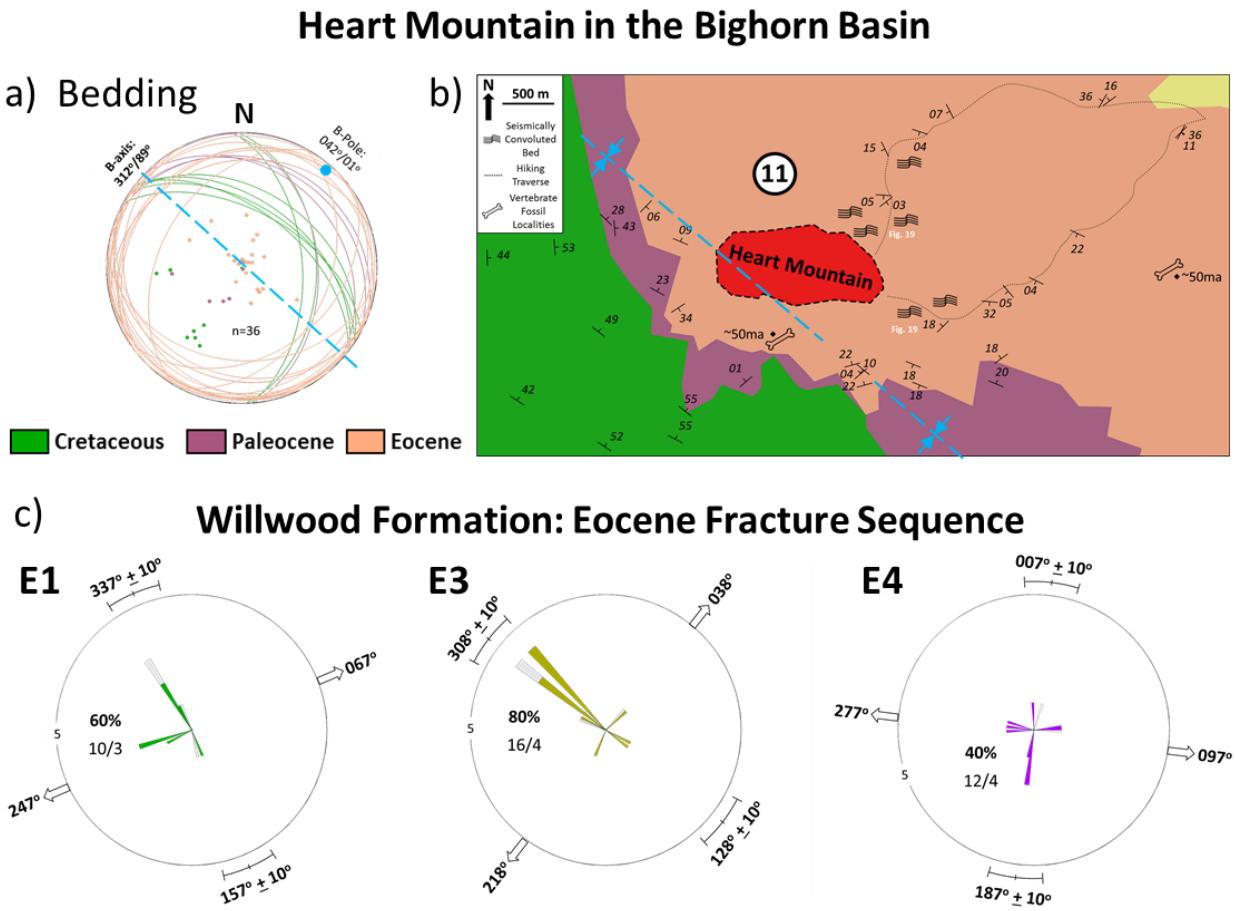

Figure 13: Heart Mountain Eocene Sequence

13a) Stereographic projection demonstrating the northwest-southeast strike trend of bedding measurements, Heart Mountain rests within a small depression/basin. The color of the bedding planes and poles-to-planes match the color of the lithologic unit on the map.

13b) Geologic map and bedding measurement along hiking traverses to the east of Heart Mountain. Bedding measurements west of Heart Mountain are from Nesser, (2014) in the Willwood and Fort Union Formations and Cretaceous units. Eocene vertebrate fossil locations from Gingerich and Clyde (2001)

13c) Rose diagrams of the Eocene fracture sequence in the Bighorn Basin Willwood Formation sediments. Rose pedals normalized to a maximum perimeter of 5 is 100%

Eocene Fractures on Dead Indian Hill

By distinguishing the Eocene fracture-sets found in the Willwood Formation allowed for recognition of additional fracture-sets in the pinned strata at Dead Indian Hill where E1 and E4 occur as joints, normal faults and reverse faults (Fig. 14). Here E1 is the prominent Eocene fracture-set, with dip-slip normal faults and reactivations of older facture sets as oblique-slip normal faults indicate NE-SW-extension (067^{o}-247^{o}). Reverse faults include a thrust fault with dip-slip direction that fit the E1-joint trend and a series of small high angle reactivations of fractures with displacement in a reverse sense with a right-lateral component. This NW-joint orientation and reverse slip-vectors of the E1-fractures are distinctly different from any NE-trending pre-Eocene fracture sets.

E2-strike-slip fractures are not recognized in the pinned strata at Dead Indian Hill and no clear primary E3-fractures were formed either, but joints and faults of pre-existing fracture-sets were reactivated as high-angle normal faults which show extension to the southwest (218^{o}) (Fig. 14). However, E4 fractures are prevalent primarily as joint-reactivation as normal faults. Some E4-joints developed in Late-Mesozoic units at Dead Indian Hill and are restricted to Chugwater to Mesa Verde strata. Here E4-joints terminate into pre-Eocene and E1-fractures. The joint arrangement matches the directions of the youngest joints at White Mountain and in the Willwood Formation (Figs. 14, 12c & 13c)

Eocene Fractures in the Allochthon

Two Absaroka dikes constrain the Eocene fracture chronology in the allochthon (Fig. 5f). Like other dikes in the detachment area, these dikes are truncated at the base by the Heart Mountain detachment fault (DeFrates et al., 2006). So, for the Eocene fracture-set (E1) which developed prior to the detachment the same vertical axis rotation may be applied to the dikes and

country rock of the allochthon, and for fractures-sets which developed after the slide the fractures remain in the present-day orientation. The northern dike margin was too weathered to acquire a confident emplacement orientation, but the southern dike strikes 307°, 82°.

Two Eocene fracture-sets are evident within the dikes. The oldest fractures are interpreted as tectonic joints in the cooled dikes pre-detachment (Fig. 15a). The strike of the oldest joints (342°) are consistent in time and orientation of E1 joints in the cooled material at White Mountain, the clastic sediments of the Willwood Formation near the Heart Mountain klippe and the sedimentary stratigraphy of Dead Indian Hill. The other joint-set, E4, occurs within the dikes as well (096°). The intermediate Eocene fracture-sets E2 and E3 are not identified in the dike outcrop.

After establishing the pre-Eocene fracture sequence in both the pinned strata and the allochthon, the younger fracture-sets were used to establish the sequence and angular relationships of Eocene fractures, just as was done for the pre-Eocene fractures (Fig. 16), in addition to the E2-strike-slip fracture-set. E1 in the allochthon is a collection of joints, normal faults, and subsequent fracture reactivations as normal faults. E1-joints trend 157°-337° $\pm$ 10°. Dip-slip and normal fault reactivations of pre-existing fractures define an extension direction of 067°-247° $\pm$ 10°. The E4 fracture-set occurs in the highly fractured allochthon as orthogonal joint-set (097°-277°/007°-187° $\pm$ 10°) identified in the post-detachment configuration of the allochthon (i.e. the present-day orientations; no angular rotations applied). Oblique-slip normal fault reactivations of all preceding fracture-sets indicate substantial collapse Dead Indian Hill west slope to the North, South and West.

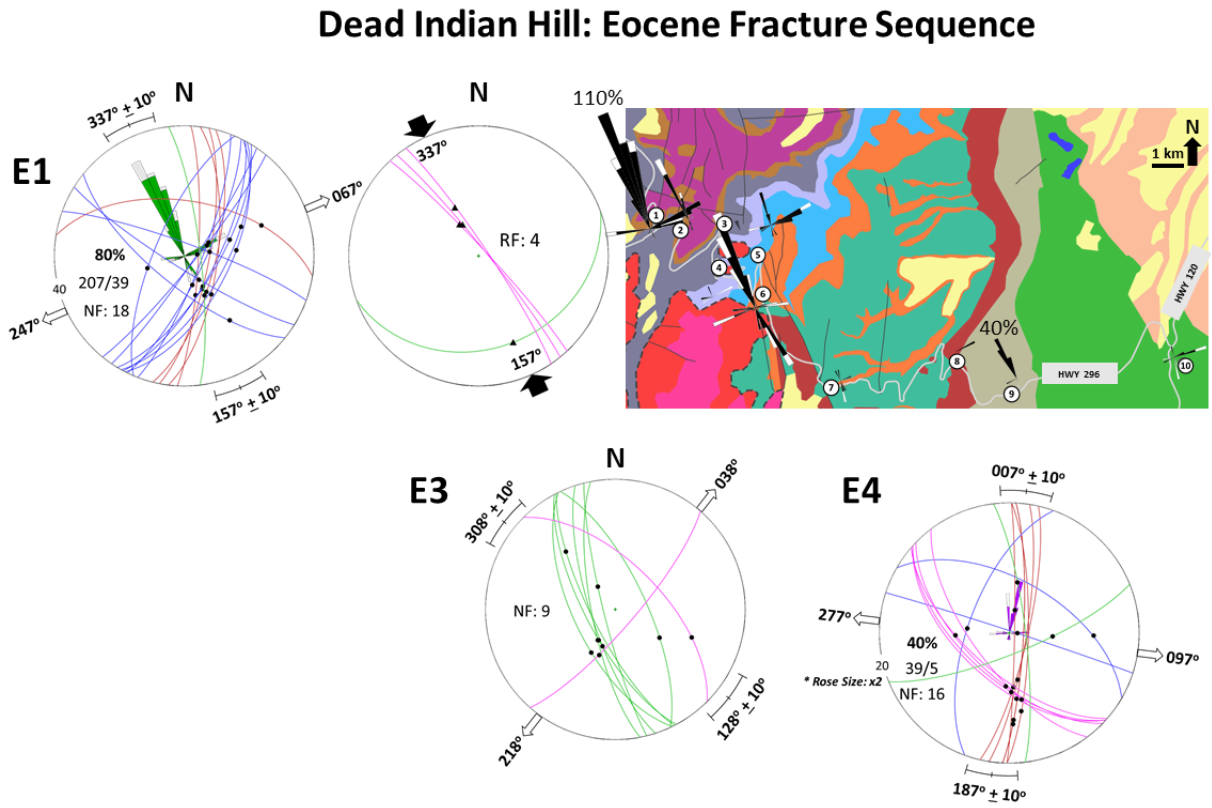

Figure 14: "Pinned" Dead Indian Hill Eocene Sequence

Stereographic projections of Eocene fractures in the "pinned" strata at Dead Indian Hill. The rows indicate sequence of events. The E1 diagrams follow the conventions of Figure 11.

*Note the E4 rose diagram perimeter is half the diameter of the Laramide and E1 diagrams

On next page *(pg.43)* →

Figure 15: The Allochthon Eocene Sequence

15a) Joint within the Absaroka dikes. E1-joints were rotated in accordance with the pre-detachment fractures. E4 joints formed after movement of the gravity-slide.

15b) The Eocene fracture sequence. Strike-slip faults are quasi-contemporaneous with the movement along the basal horizon. E2-fracture subsets, E4-fractures are plotted in the present-day orientation (i.e. unrotated or post-detachment) versus E1-fractures. Red and yellow lines (matching the secondary antithetic fractures in Figure 8) are approximate fit lines of the plunge and plunge azimuth of the lineation of the fracture surfaces.

Faults: solid squares are Left-Lateral, hollow squares are Right-Lateral, and dots are normal faults plotted to the right.

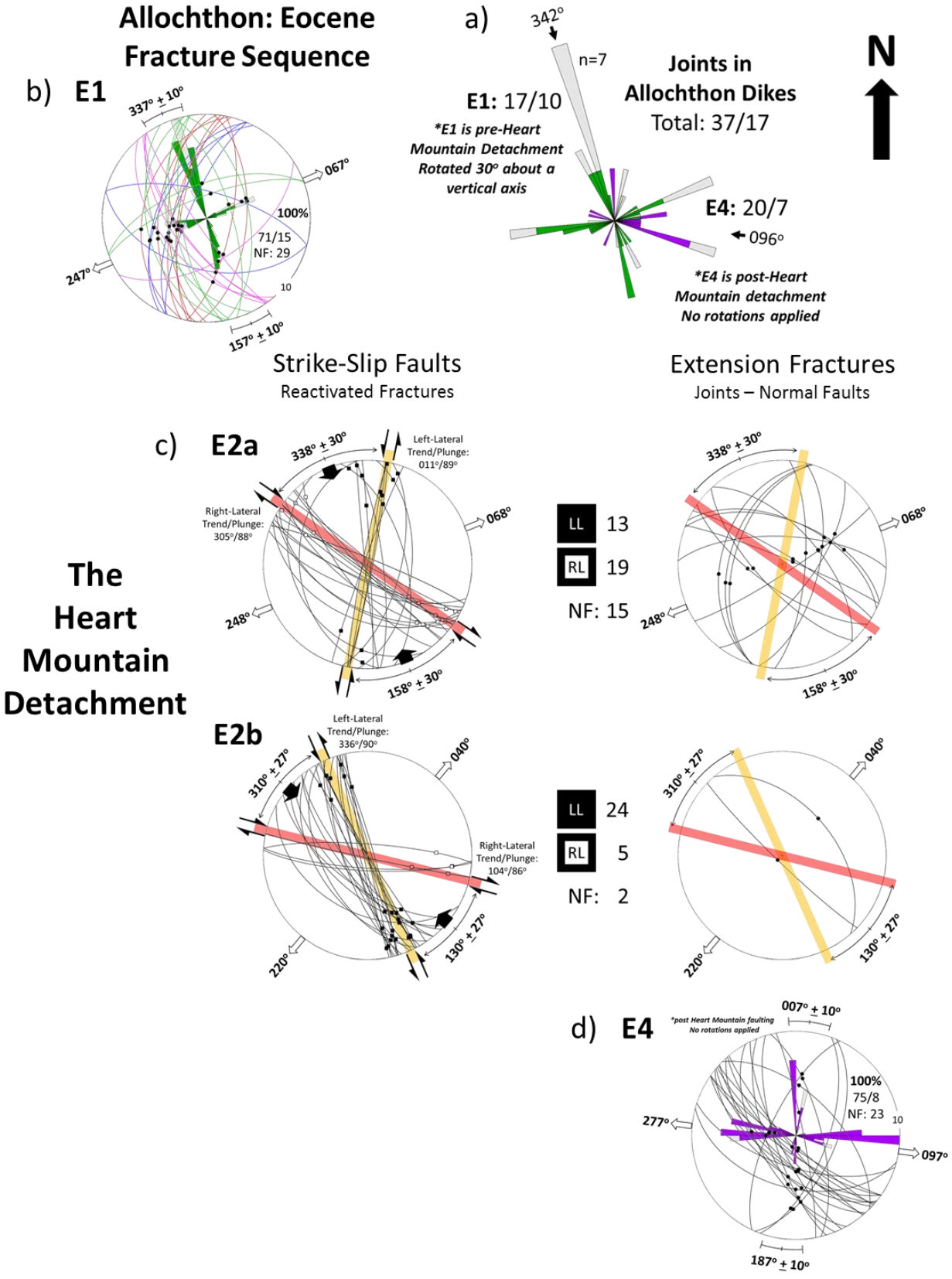
Allochthon: Eocene Fracture Sequence
a)
342°
n=7
Joints in Allochthon Dikes
Total: 37/17
N
E1: 17/10
*E1 is pre-Heart Mountain Detachment Rotated 30° about a vertical axis
E4: 20/7
096°
*E4 is post-Heart Mountain detachment No rotations applied
b) E1
337° ± 10°
067°
100%
71/15
NF: 29
10
247°
157° ± 10°
Strike-Slip Faults
Reactivated Fractures
Extension Fractures
Joints – Normal Faults
The Heart Mountain Detachment
c) E2a
338° ± 30°
Left-Lateral Trend/Plunge: 011°/89°
068°
Right-Lateral Trend/Plunge: 305°/88°
248°
158° ± 30°
LL 13
RL 19
NF: 15
E2b
Left-Lateral Trend/Plunge: 336°/90°
040°
310° ± 27°
Right-Lateral Trend/Plunge: 104°/86°
220°
130° ± 27°
LL 24
RL 5
NF: 2
d) E4
*post Heart Mountain faulting No rotations applied
007° ± 10°
100%
75/8
NF: 23
10
277°
097°
187° ± 10°

Eocene Strike-Slip Faults in the Allochthon

The E2 fracture-set was observed only along the western slope of Dead Indian Hill and is an assembly of reactivated fractures (primarily joints) as strike-slip faults and oblique-normal faults. No new joints or normal faults formed as a part of E2. In the allochthon, E2 is defined by a series of strike-slip faults developed where the bisecting direction of the dihedral angle of the right-lateral and left-lateral joint-reactivations are orientated NW-SE and NNW-SSE and complementary normal faults which indicate lateral extension direction 90^{o} away from the bisecting angle of the strike-slip conjugate pairs (Fig. 15c). The first sub-set (E2a) of strike-slip fault system has a bisector oriented the same as the E1-joints (158^{o}-338^{o}), but must be inferred as a younger fracture set because E1-joints and normal faults in the allochthon are in an orthogonal "stress-switching" pattern which would unconducive for strike-slip faulting. E2a oblique-normal fault reactivations of pre-existing fractures define an extension direction of 068^{o}-248^{o}, which is like E1-normal faults. The second subset of strike-slip (E2b) reactivations have a counterclockwise rotation 28^{o} of the bisecting angle oriented (130^{o}-310^{o}), which is similar to the E3-joint trend in the cooled fault breccia at White Mountain, below the Heart Mountain klippe in the basin, and the southwestern extension of E3-normal faults in the sub-detachment Dead Indian Hill stratigraphy.

DISCUSSION

Seven fracture-sets found within the Heart Mountain detachment area (Table 1 & Figure 16, 17) provide a timeline and suggest possible modes of deformation at Dead Indian Hill. The sequence of meso-scale brittle fractures presents tectonic events leading into and related to the Laramide Orogeny (PL1, L1, L2) and to the regional thermal expansion and subsequent collapse

of the Northeastern Absaroka Volcanic Province edifice, including the Heart Mountain detachment (E1, E2, E3, E4).

As noted previously, a key idea in this study is the concept of "stress-switching" in the foreland of emerging subsurface thrust faults (Bartholomew and Whitaker, 2010) or expansion of a thermal bulge due to an increase of the crustal heat flux (Koide and Bhattacharji, 1975). "Stress-switching" creates the orthogonal joint pattern caused by the bending moment stress, when an extensional environment develops across the outer surface of a peripheral arch or bulge. If the controlling fault is a subsurface reactivation of a basement fault (as many Laramide structures are interpreted to be (Bump, 2003)), an appropriate ratio of slip to fault length must be achieved before a basement fault to propagate lengthwise towards surface (Bellahsen et al., 2006). The "stress-switching" joint pattern in the research area could manifest in three forms and by no means is limited to a singular mechanism:

1) Near equivalent horizontal stress values – Incremental changes of magnitude between nearly equal horizontal principle stress values can switch the extension direction of fractures (σ_3). When σ_1 is vertical and the magnitude of σ_2/σ_3 are nearly equal, then minor perturbations of the stress field may invert the orientations of σ_3 and σ_2 rotating the opening detection of fractures 90^o (Bai et al., 2002).
2) Local rotation of the stress field following joint formation – Upon the formation of a joint the local stress field can flip 90^o at the individual joint scale (Dunne et al., 2003).
3) Regional rotation of the stress field – Switching on the regional scale occurs due to the stress state change related to tectonic influences over time or consequential relaxation of stress following uplift and/or erosion (Dunne et al., 2003).

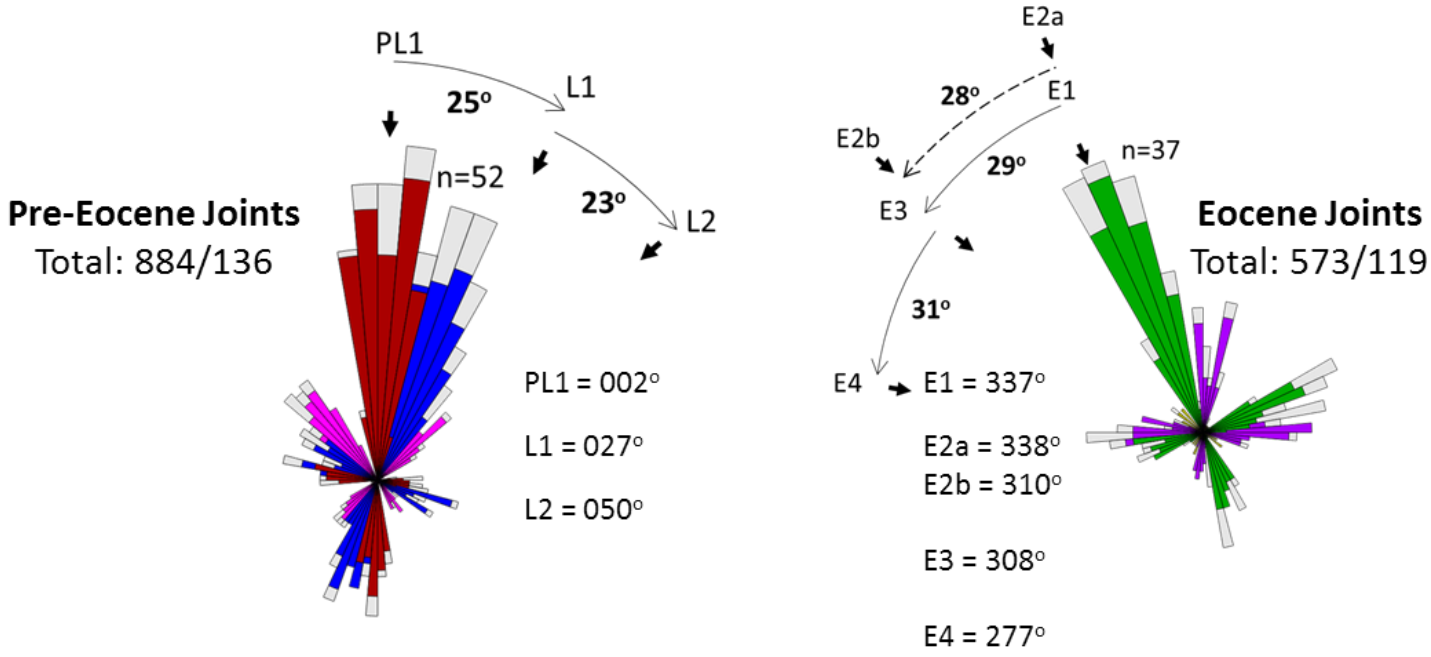

Figure 16: Pre-Eocene and Eocene Joint Sequence

Rose diagrams (azimuth, 0° -360°, measured by right-hand-rule) of the Pre-Eocene and Eocene joint sequence. The black arrows are the mean orientation of each fracture set. The arched arrows are the rotation magnitude and direction of the maximum principle horizontal stress of each fracture set. Each sequence shows the reliable abutting and angular arrangement of joints as the principle stresses rotate through time and allows for the correlation of joints to tectonic events. The Pre-Eocene fracture sequence is a clockwise rotation of 50° E from the north in Paleozoic and Mesozoic strata. The Eocene fracture sequence is a counterclockwise rotation from 337° W to 308° W in all strata. The dashed arch is the rotation of the strike-slip faults of the Heart Mountain detachment which correlates well with the end member E1 and E3 fracture sets.

Pre-Eocene Sequence

(Pre-Laramide and Laramide Sequence)

Laramide events agree with orogenic stress trend in the Montana and Wyoming region (e.g., Gries, 1983; Dickenson et al., 1988; Erslev, 1993; Bird, 1998; DeCelles, 2004), as well as specifically in the adjacent Laramide structures to Dead Indian Hill (Wise and McCrory, 1982; Beutner and DiBenendetto, 2003; Bellahsen et al., 2006; Neely and Erslev, 2009; Beaudoin et al., 2012; Neser, 2014; Jackson et al., 2016). The two Laramide fracture-sets in the central portion of the Dead Indian Hill fold limb show a clockwise rotation of the principle stress orientations from NNW-SSE-compression (σ_1 or H_{max}) (E-W-extension (σ_3)) to NE-SW-compression (σ_1) (SE-NW-extension (σ_3)) (Fig. 10, 11c, 16a, 17).

PL1 is well defined by N-trending joints (Table 1 & Figure 17) which are strongly developed in the Flathead Formation that is pinned to basement in Sunlight Valley (Figs. 10 & 18). Throughout Paleozoic strata near Dead Indian Hill, N-trending PL1 joints remain the dominant fracture, although in a few locations $PL1_o$ is well developed (Fig. 10). In the Flathead Formation (Location 1 & 6) PL1 joints are perpendicular to bedding and extend vertically across the bed thickness in an en echelon arrangement to one another. The en echelon arrangement and slip vectors of PL1 dip-slip normal faults indicate E-W-extension (σ_3).

L1 and L2 (Fig. 10) represent a bi-modal fracture sequence of NE-SW-compression highlighted by conjugate thrust faults and reactivated thrust faults which match Laramide slip-vector trends (Neely and Erslev, 2009). L1 and L2 joints abut into PL1-fractures and PL1-fractures were reactivated as oblique-slip normal faults under the stress regimes of the L1 and L2 events in Cambrian through Permian strata. In Triassic through Mid-Cretaceous rocks L1-fractures become the oldest fracture set in that part of the sedimentary record indicating a tectonic shift from a passive margin toward active mountain building in northwestern Wyoming

(Fig. 10). In the present-day folded configuration, young joints and fault-reactivations which are in the same orientation as PL1 abut into adjacent fractures and therefore are considered the product of E4, which had a similar principle stress orientation as PL1, but is a significantly younger deformation event.

The passage from passive PL1 deformation (where σ_1 is vertical) to compressive L1 (where σ_1 is horizontal) signifies the beginning of significant Laramide deformation in northwestern Wyoming (Gries, 1983) marked by a horizontal clockwise 25^o rotation of the stress field (Fig. 16a) The L1 joint-set (Table 1) (027^o-207^o $\pm$ 10^o) agrees with the initial Laramide joint orientation joints collected in Cretaceous units at Hogan reservoir (020^o, Neser, 2014), and generally with reported at the Rattlesnake Mountain Anticline to the south (030^o-070^o, Beaudoin et al., 2012). The orientation of conjugate L1-reverse fault planes and the azimuth of the plunge the slickenlines (Table 1 & Figure 10) (026^o and 205^o) are consistent with the principle joint orientation L1-joints, signifying at the time of faulting σ_1 was positioned in a near horizontal plane. Like PL1, L1 at certain localities has an orthogonal relationship of joints and normal faults that suggest pre-thrust arching of the foreland before a subsurface thrust fault had propagated to the near surface (Fig. 10).

The second phase of active Laramide tectonism at Dead Indian Hill, L2 is a clockwise rotation of the principle stresses 22^o away from L1-fractures (48^o from PL1 fractures) (Fig. 16a). Reverse faults and reactivations of L1-thrust faults during L2 (azimuth of the plunge the slickenlines – Primary: 233^o & 234^o Reactivations: 053^o & 230^o) display continued Laramide NE-SW- compression (σ_1) in Northwestern Wyoming (Fig. 10). These fault plane orientations and slip-vectors at Dead Indian Hill correspond with the ~300^o fault plane trend of faults elevated on the Beartooth Plateau (Foose et al., 1961), the Blacktail thrust-fold (fold-axis trend 310^o-330^o

NW) in the Cambrian units below detachment in the "Bedding-Parallel" area (Beutner and DiBenendetto, 2003), as well as, on striated micro-faults at Rattlesnake Mountain (striation azimuth: 035°-050°, Beaudoin et al., 2012). L2 has the strongest orthogonal extension pattern of the Laramide fracture-sets, indicating a more common occurrence of "stress-switching" as curvature of the Dead Indian Hill arc increases (Fig. 10 & 17).

Eocene Sequence

Development of the Absaroka Volcanic Province was related to regional thermal expansion, an elevated thermal gradient, and volcanic eruptions. As in other large volcanic fields in western North America, radial dike patterns often delineate volcanic centers as in the Absaroka Province (Koide and Bhattacharji, 1975), where σ_1 is approximately vertical. Here, $^{40}Ar/^{39}Ar$ ages place two centers at 50.1-48.1ma (New World Mining District; Douglas et al., 2003) and 49.6-48.1ma (Sunlight Volcano; Feeley and Cosca, 2003). Obviously, new fractures that developed within Absaroka dikes are Eocene or younger. But for a first approximation, σ_1 is considered vertical for the domal centers to the west and south of the pinned Laramide structures and no correction for bedding was used. As with the Pre-Laramide and Laramide fracture sequence, the same methods (abutting joint relationships and angular relationship between joints) were used to elucidate the unique Eocene fracture sequence (Fig. 16b). Intrusion of dikes and sills within domal centers likely contributed to inclined detachment plane (Aharonov and Anders, 2006, Anders et al., 2010, Swanson et al., 2016). The two dikes (Fig. 5f) in the allochthon at Dead Indian Hill, are likely truncated by the detachment fault. Because dikes can dilate pre-existing fractures in rock (Delaney et al., 1986) they are not always reliable indicators of the regional stress state at the time of emplacement. The margin of the southern dike (307°, 82°) appears to follow a pre-existing fracture ($L1_o$: 117°-297° $\pm$ 10°) (Fig. 5f). The sequence of

fracture-sets and the angular arrangement of Eocene fracture-sets show the sequence west of Dead Indian Hill was accompanied by local build-up collapse of an Absaroka volcanic system in northwestern Wyoming (Fig. 16b).

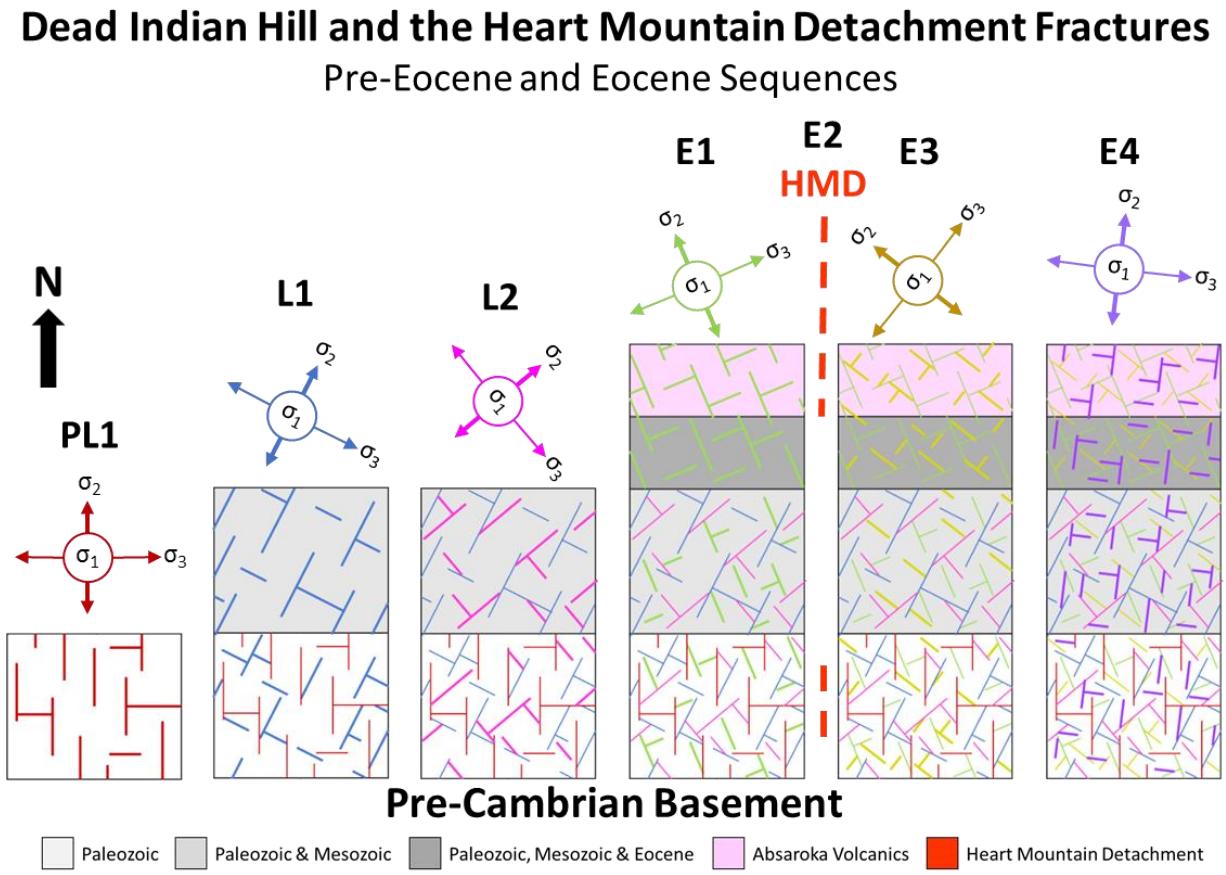

Figure 17: All Joint Sets

Joint evolution in the Dead Indian Hill area. Joint patters, the result of the bending moment stress, as the Dead Indian Hill fold matured throughout the Laramide Orogeny (PL1, L1, L2) and the build-up of the Absaroka Volcanic Province (E1), followed by the ensuing collapse of the northeastern Absaroka (E3 & E4). No joints formed with E2.

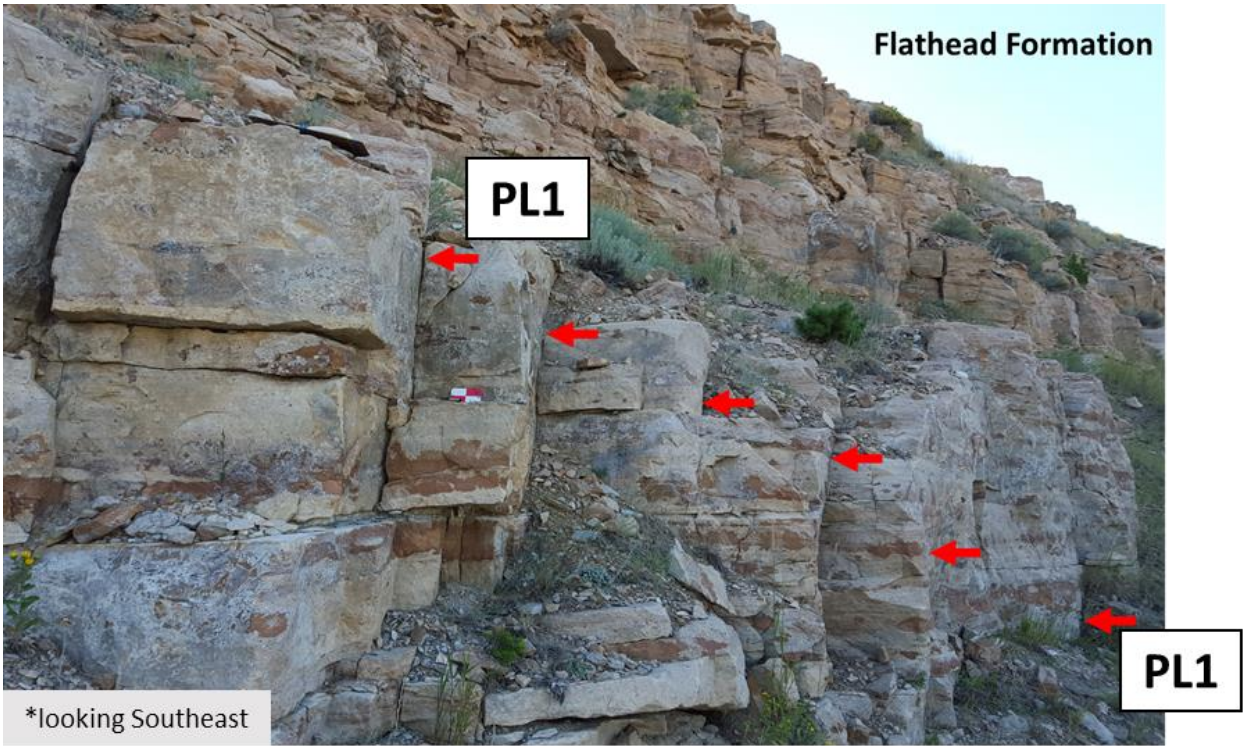

Figure 18: PL-1 Joints

The prominent PL1-joints in the Cambrian Flathead Formation which is "pinned" to the Pre-Cambrian crystalline basement. The en echelon fanning of the PL1 joints (which are oriented roughly N-S) indicates extension in the E-W direction.

A) Pre-Detachment Eocene Sequence

E1 is the most consistent fracture-set in the Heart Mountain detachment area (Fig. 17). The dominant NW-SE-joint trend occurs in all rock types and all areas, observed in: 1) "pinned" strata; 2) the allochthon with Absaroka dikes; 3) at White Mountain; and 4) in the Willwood Formation. In the igneous intrusions and thermally altered wall rocks, E1-joints are systematically the oldest and largest fractures. The allochthon dikes have NW-trending E1-joints (342^o) with a very minor $E1_o$. This NW-joint trend corresponds with E1-joints in the Willwood Formation which form the oldest (Early-Eocene) fracture-set, with a Late-Wasatchian age (~50ma; Gingerich, 1983) proximal to the Heart Mountain klippe. A diverse collection of stratigraphic and geochemical research refines the temporal sequence of individual units related to the Heart Mountain detachment in the Eocene (e.g., Malone et al., 2014). E1-joints trend NW near Dead Indian Hill (157^o-$337^o \pm 10^o$) where slip-vectors match the reverse fault and oblique-reverse high-angle fractures (azimuth of the plunge the slickenlines – Primary: 158^o Reactivations: 329^o, 333^o & 334^o) below the detachment; hence σ_1 was horizontal at Dead Indian Hill. $E1_o$ represents a minor, unevenly distributed population of joints, dip-slip normal faults, and oblique-slip reactivation of normal faults. $E1/E1_o$ are suggestive of stress-switching across the extensional domal surface of the Absaroka bulge as the slope steepened along the eastern flank of the volcanic center. At White Mountain, $E1/E1_o$ form a prominent fracture-set consistent with a swelling thermal bulge and eruptions of thick volcanics over the exhumed Paleozoic carbonate platform. This NW- trending E1-joint-set coupled with ~60^o dip-slip normal faults are consistent with a NE-SW-extension direction (σ_3) (Figs. 12c, 13c, 14, 15b) although, no slip-indicators were noted on these meso-scale faults. The variability of $E1_o$-joint development across the regional strata may be a function of how joints had formed in different

localities along the detachment perimeter or may be related the thickness of the volcanic overburden around the volcanic centers.

B) Heart Mountain Detachment Eocene Sequence

Considering that fault-slip vectors in the allochthon indicate the detachment moved NNW-SSE along the steep western flank of Dead Indian Hill rather than eastward as depicted in the classic interpretations then a different transport model is required and presented herein. The relief at the west slope of Dead Indian Hill may due to the rapid collapse of the northeastern Absaroka edifice against the "pinned" and rigid Dead Indian Hill and the Beartooth Plateau orogenic platform rather than a pre-established ramp prior to detachment.

As Absaroka eruptions continued, E1 "stress-switching" weakened the domal surface of the Absaroka bulge and the Heart Mountain gravity-slide was triggered and transported as strike-slip and oblique-normal faults along pre-existing fractures. E2 consists of NW-SE conjugate strike-slip and vertical oblique-normal faults which are reactivated joints in Paleozoic units in the allochthon (Fig. 15b). Two E2-fracture subsets (Fig. 16b) of strike-slip faults indicate a (southward) counterclockwise 28^{o} rotation of the σ_1 orientation, defined by the line which bisects dihedral angle of the conjugate pairs. These E2-subsets (collapse) likely happened in rapid succession as the northeastern slope of the Absaroka edifice failed following E1-extension

E3 orthogonal joints and normal faults likely developed as the resultant stress-field following the strike-slip faults of the detachment event (E2) and led to emplacement of the detachment sheet southeast of the Laramide front which are now preserved as the Heart Mountain and McCullough klippe. The NW-trending E3-joints and normal faults (128^{o}-308^{o} $\pm$ 10^{o}) show a 29^{o} counterclockwise relative to E1 which is near the same rotation between the E2-sub-sets (Fig. 16b).

This ~30º rotation of the stress-field and sliding of the Heart Mountain detachment sheet could perhaps have been caused by the rise of a new volcanic center (Malone et al., 2017), an increase of eruptive activity at an individual volcano (Beutner and Gerbi, 2005), sector collapse of a large volcano (Craddock et al., 2009) and/or thermal relaxation of the entire northeastern Absaroka volcanic field. Eocene normal faults and joints at White Mountain and the allochthon (Fig. 12c, 15b & 16), E3-normal faults below the detachment in the pinned Dead Indian Hill (Fig. 14) and E3-joints in the Willwood (Fig. 13) show a NE-SW-extension direction (σ_3). Based on the widespread E1 and E2a-extension directions (σ_3) in the allochthon (location 12 & 13, Figure 4 & 15b) west of Dead Indian Hill, the lack of faults which indicate any type of reverse motion in the Eocene, the E3-joint opening direction (σ_3) and the position of the Heart Mountain klippe (location 11, Figure 4 & 13) in the NW-SE-trending Eocene trough, it is unlikely that the klippe slid southeastward up the western slope of Dead Indian Hill and then over the top of the "pinned" Late-Paleozoic and Mesozoic strata there as often depicted (Pierce, 1957, Hauge, 1993, Anders et al., 2010). Thus, the Eocene extension directions are consistent with a new interpretation that the Heart Mountain klippe originated from the direction of Rattlesnake Mountain (Fig. 15b).

Stratigraphically below the Heart Mountain klippe, multiple thick Willwood sandstones (> 5m) are highly convoluted and laterally extensive around the northern fringe of the mountain (Fig. 19). Similar convolute bedding has been described, several kilometers to the northwest, in thick channel sandstones near the base of the Willwood Formation and is linked with different types of paleoseismites (clastic dikes, sand blows and other liquefaction features) related to the Laramide uplift of the Beartooth Plateau, in the underlying Paleocene Fort Union Formation (DeCelles et al., 1991; Bartholomew et al., 2008; Stewart et al., 2008). Likewise, clastic dikes,

convolute bedding, and other paleoseismites occur in Cretaceous sandstones in the northern Bighorn Basin attributed to the progressive development of the Elk Basin anticline (Jackson et al., 2016). Accordingly, the large Eocene paleoseismites found immediately below Heart Mountain likely reflect emplacement of the Heart Mountain klippe into the basin (Fig. 19). The western dip of the Willwood Formation beds to the east of the Heart Mountain klippe may too be a be a local product of the emplaced lithostatic load of the Paleozoic klippe on the saturated sandstone basin floor. Further, mapping of the Eocene section east of the mountain could resolve if the Eocene surface is a part of a larger fold.

Figure 19: Willwood sandstone Paleoseismites

Thick and continuous paleoseismites surrounding the northern base of Heart Mountain, Bighorn Basin. Water saturated beds of Willwood Formation sandstones may be heavily convoluted and overturned by seismic or lithostatic pressures caused by the emplacement of the Heart Mountain mass.

C) Post-Detachment Eocene Sequence

From the summit of Dead Indian Hill (EL. 2460m) to Sunlight Valley (EL. 1875m) lies the classic "transgressive-ramp" of the detachment fault, where the hanging wall of the basal fault allegedly ramps up-section into the Bighorn and Madison Formations. (Fig. 20). The allochthon sits dipping ~30^{o} NW (Mean Bedding Plane Orientation - Madison: 235^{o}, 30^{o} and Bighorn: 274^{o}, 31^{o}) on the shallowly SE-dipping Bighorn Dolomite (Fig. 11a,b), but, as mapped at other locations throughout Sunlight Valley, the klippe sit directly on pinned Cambrian strata under the detachment. High-angle normal faults with significant offset bound the block of pinned Cambrian strata (Wise and McCrory, 1982) (Fig. 4, 20). South of the summit the detached beds of Bighorn and Madison masses are chaotically W-, S-, and N-dipping with various inclinations (Fig. 20). The Tectonic Denudation Model uses landslides onto the exposed fault surface as the cause of bed dips (Pierce, 1957). Instead, these dipping beds appear to be bounded by large-scale normal faults (as Hauge (1990) had interpreted, although these faults developed in a post-detachment setting and not contemporaneous with the detachment). Unlike the Tectonic Denudation and Continuous Allochthon models, the erratic and discordant dips of the carbonate beds are related to thermal subsidence of Sunlight Valley on the northeastern fringe of the detachment sheet.

E4 is the youngest fracture-set in the study area. E4-joints are only a minor population in the Late-Mesozoic and Willwood sediments. At White Mountain (Location 14) E4-joints strike north and abut into the E1 and E3 fractures in the altered Bighorn Dolomite and fault breccia. Few identifiable E4-joints formed in the sub-detachment strata of the on the west slope of Dead Indian Hill, which primary deformed by reactivations of pre-existing joints and normal faults.

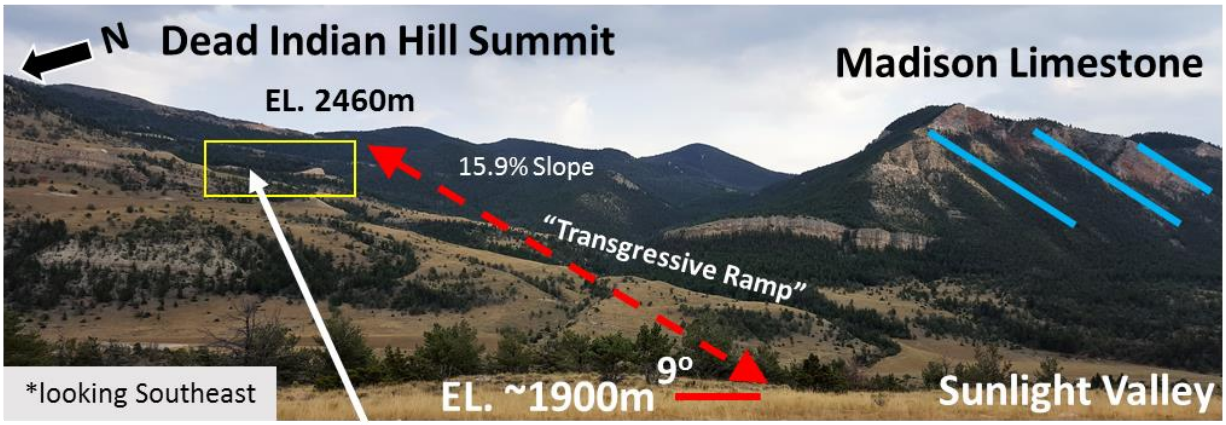

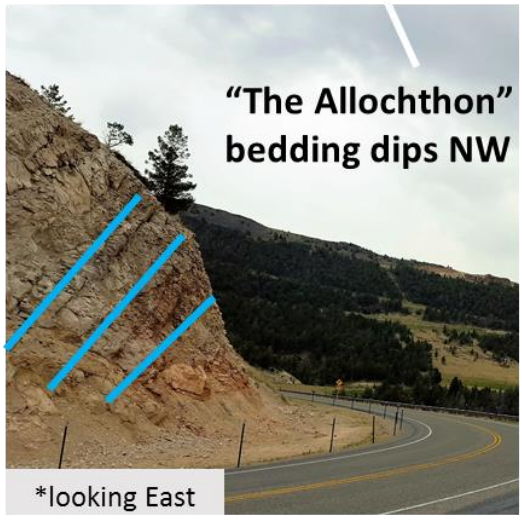

Figure 20: West Slope of Dead Indian Hill

Chaotic Paleozoic carbonate beds dipping in various directions and inclinations, away from Dead Indian Hill and into the Sunlight Valley. At the "Transgressive Ramp" the bedding of the Paleozoic beds dip in opposing directions into the hill an atop the Cambrian units in Sunlight Valley.

The "pinned" Dead Indian Hill stratigraphy, the Willwood Formation, and White Mountain, all areas which have shallow sub-horizontal dipping beds, all have the orthogonal E4 joint pair (Fig. 17). In the allochthon at Dead Indian Hill, joints in the orthogonal pattern of E4 (Fig. 15b) were only recognizable in a dataset of present-day vertical fractures. When executing a fold-test for the pre-detachment fractures in the allochthon (restoring the allochthon to the pre-detachment position), E4-fractures were differentiated from the pre-detachment fractures because the E4-fractures had rotated to dips less than 65^{o}. This group of fractures indicated they formed in the allochthon post-detachment and after the allochthon had come to rest on the hillslope. Also, these joints agree with the youngest joints at White Mountain, the Willwood formation and in the Mesozoic Dead Indian Hill strata.

E4 fractures are abundant open orthogonal joints and normal faults along the hillcrest of Dead Indian Hill (HWY 296, Location 6) and appear to have formed by topographic collapse during the youngest event. Prior to excavation of this new roadcut, a 1-2m-thick siliceous breccia with abundant large (5-10cm) voids was mapped along the approximately horizontal upper contact of the Tensleep Formation (Fig. 21) for ~0.5km along the ridge crest. To the east ~0.5km across the fold crest a similar siliceous breccia, dips moderately eastward indicating that this folded breccia formed during Laramide deformation. Similar 1-2m thick breccia zones also occur lower in Tensleep section in this roadcut. This ~20m-tall road-cut of Pennsylvanian Tensleep Formation (Fig. 21) was highly fractured and broken into small discrete blocks of sandstone. Normal faults in the sandstone are reactivated joints that became high-angle normal faults near the surface. Below the Tensleep Formation, the "pinned" Madison Limestone on both sides to the hillcrest appears to be collapsing (Fig. 22).

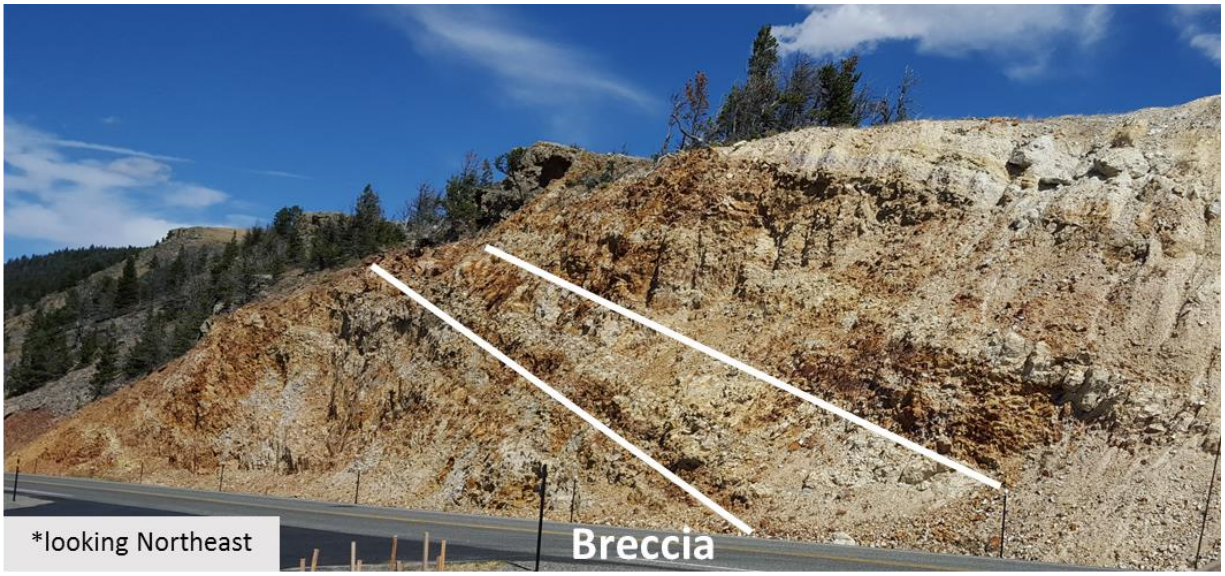

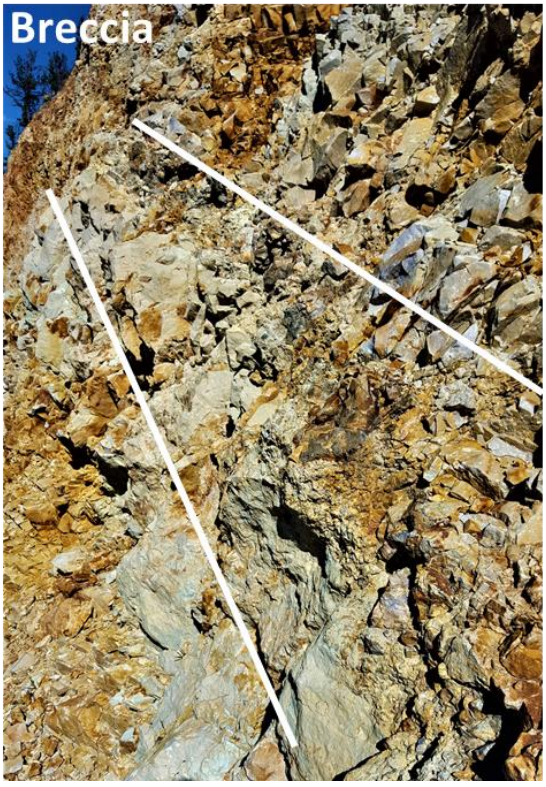

Figure 21: Tensleep Formation at the Dead Indian Hill Summit

Heavily fractured and brecciated sandstone of the Tensleep. Fracture 1m thick siliceous breccia which pre-dates the Heart Mountain detachment. Abundant open fractures create discrete sandstone blocks loosely fitted together in the outcrop.

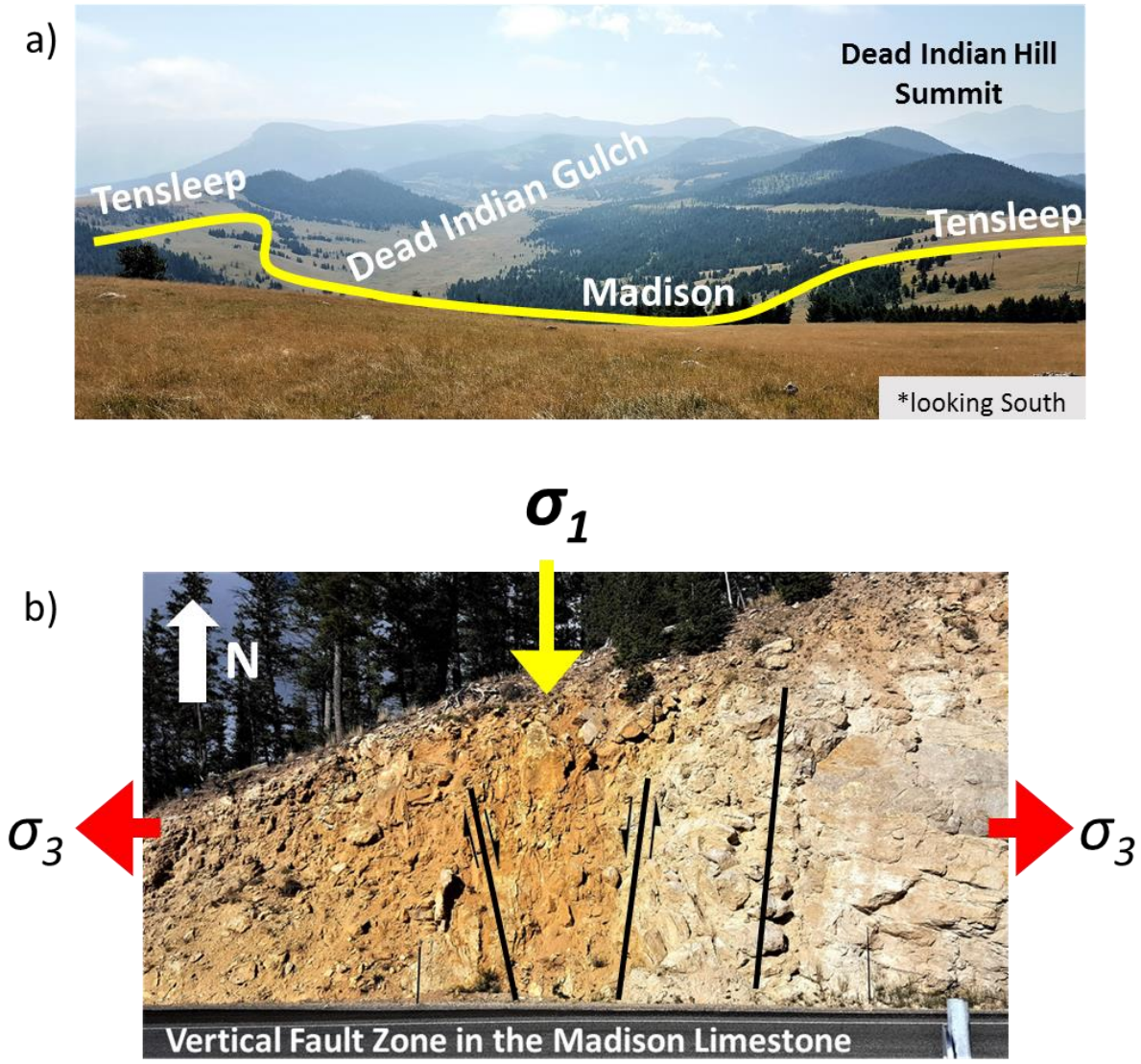

Figure 22: Collapse Features at Dead Indian Hill

a) Dead Indian Gulch. Gravitational collapse of the hillcrest of Dead Indian Hill.

b) Reactivated fracture as a high-angle normal fault in the Madison Limestone near the "pinned" Dead Indian Hill summit. The footwall (orange zone) is down to the west or towards the Sunlight Valley.

To the east of the hillcrest, the Dead Indian Gulch (Fig. 4 & 22a) is a graben within the limestone separating two ridges of the Tensleep Formation. The depression trends NNE in the Madison Limestone, sloped down towards the Clarks Fork River. This trend matches the extension direction (σ_3) of the N-S-set (E4) as well as strikes in the same orientation as mapped vertical faults on the east slope of Dead Indian Hill (Pierce, 1965a; Pierce and Nelson, 1968), and the large klippe atop the Dead Indian Hill looks to be collapsing into the graben as well (Fig. 22a).

West of the hairpin of HWY 296 (Location 5) a vertical ~5m-wide, N-trending, heavily argilized fault zone in the Madison Limestone (Fig. 22b), which aligns with near vertical normal faults mapped at the Dead Indian Hill summit (Pierce, 1965a; Pierce and Nelson, 1968). Overprinting of surface minerals and unique crystal growths coat fracture surfaces but, due to intense argilization, chaotic mélange of fallen rock, and infill of void spaces by unconsolidated sediment precludes determining if any fractures are preferential mineralized.

Conclusion

The meso-scale brittle fracture framework of joints and faults found within the Heart Mountain detachment and the underlying pinned stratigraphy is remarkably consistent. Major tectonic events were identified by the investigation into the fracture frameworks spanning from the Cambrian to Eocene. Based upon the abutting and angular relationships of joints, reactivation of pre-existing fractures as faults in subsequent stress fields and joint development in chronostratigraphic horizons, we isolated the passive lead into the Laramide Orogeny (PL1), the active orogenic thrusting of the Laramide Orogeny (L1 & L2), the thermal expansion of the crust brought on by the Absaroka Volcanic Province (E1), the rapid transport of the Heart

Mountain detachment and collapse of the northeastern Absaroka edifice and the continued post-detachment extension throughout the area.

The angular relationship and gross population joint-sets led to not just identification of Pre-Eocene and Eocene fracture patterns but also allowed us to quantify ~30^{o} counter clockwise vertical axis rotation of the allochthon on the slope of Dead Indian Hill. Eocene bedding and fracture data suggests the allochthon was transported in southeast direction. However, vertical joints reactivated as strike slip and normal faults show neither the detachment sheet nor the Heart Mountain klippe "ramped" up and over the backslope of Dead Indian Hill. The Heart Mountain klippe likely originated near Rattlesnake Mountain. The present relief of the "transgressive ramp" is a post-detachment feature caused by the failure of the northeastern Absaroka edifice and the thermal subsidence of Sunlight Valley as the Absaroka thermal bulge relaxed.

References

Aharonov, E., and Anders, M. H., 2006, Hot water: A solution to the Heart Mountain detachment problem?: Geology, v. 34, no. 3, p. 165-168.

Allmendinger, R. W., Gephart, J. W., and Marrett, R. A., 1989, Notes on fault slip analysis, Volume Prepared for the Geological Society of America Short Course on "Quantitative Interpretation of Joints and Faults".

Anders, M. H., Christie-Blick, N., and Walker, C. D., 2006, Distinguishing between rooted and rootless detachments: A case study from the Mormon Mountains of southeastern Nevada: Journal of Geology, v. 114, no. 6, p. 645-664.

Anders, M. H., Fouke, B. W., Zerkle, A. L., Tavarnelli, E., Alvarez, W., and Harlow, G. E., 2010, The Role of Calcining and Basal Fluidization in the Long Runout of Carbonate Slides: An Example from the Heart Mountain Slide Block, Wyoming and Montana, U.S.A: Journal of Geology, v. 118, no. 6, p. 577-599.

Bai, T., and Gross, M. R., 1999, Theoretical analysis of cross-joint geometries and their classification: Journal of Geophysical Research, v. 104, no. B1, p. 1163-1177.

Bai, T. X., Maerten, L., Gross, M. R., and Aydin, A., 2002, Orthogonal cross joints: do they imply a regional stress rotation?: Journal of Structural Geology, v. 24, no. 1, p. 77-88.

Bartholomew, M. J., Stewart, K. G., Wise, D. U., and Ballantyne, H. A., 2008, Field guide; Paleoseismites; indicators of Laramide tectonism and other events near the Bighorn Basin, Montana and Wyoming: Northwest Geology, v. 37, p. 135-158.

Bartholomew, M. J., and Whitaker, A. E., 2010, The Alleghanian deformational sequence at the foreland junction of the Central and Southern Appalachians: From Rodinia to Pangea: the Lithotectonic Record of the Appalachian Region, v. 206, p. 431-454.

Beaudoin, N., Lepretre, R., Bellahsen, N., Lacombe, O., Amrouch, K., Callot, J.-P., Emmanuel, L., and Daniel, J.-M., 2012, Structural and microstructural evolution of the Rattlesnake Mountain Anticline (Wyoming, USA): New insights into the Sevier and Laramide orogenic stress build-up in the Bighorn Basin: Tectonophysics, v. 576, p. 20-45.

Bellahsen, N., Fiore, P., and Pollard, D. D., 2006, The role of fractures in the structural interpretation of Sheep Mountain Anticline, Wyoming: Journal of Structural Geology, v. 28, no. 5, p. 850-867.

Beutner, E. C., and Craven, A. E., 1996, Volcanic fluidization and the Heart Mountain detachment, Wyoming: Geology, v. 24, no. 7, p. 595-598.

Beutner, E. C., and DiBenedetto, S. P., 2003, The Blacktail thrust-fold, Crandall Conglomerate, and Heart Mountain detachment fault, northwestern Wyoming: Rocky Mountain Geology, v. 38, no. 2, p. 237-245.

Beutner, E. C., and Gerbi, G. P., 2005, Catastrophic emplacement of the heart mountain block slide, Wyoming and Montana, USA: Geological Society of America Bulletin, v. 117, no. 5-6, p. 724-735.

Biek, R. F., Hacker, D. B., and Rowley, P. D., 2016, Catastrophic Mega-Scale Landslide Failure of Large Volcanic Fields, GSA Today, Volume VOL. 26: Boulder, CO, The Geological Society of America® Inc., p. 22-24.

Bird, P., 1998, Kinematic history of the Laramide orogeny in latitudes 35 degrees-49 degrees N, western United States: Tectonics, v. 17, no. 5, p. 780-801.

Blackstone, D. L., Jr., 1986, Structural geology, northwest margin, Bighorn Basin; Park County, Wyoming and Carbon County, Montana: United States, Yellowstone Bighorn Research Association, United States, p. 125-135.

Bucher, W. H., 1947, Heart Mountain problem, p. 189-197.
Craddock, J. P., Malone, D. H., Magloughlin, J., Cook, A. L., Rieser, M. E., and Doyle, J. R., 2009, Dynamics of the emplacement of the Heart Mountain allochthon at White Mountain: Constraints from calcite twinning strains, anisotropy of magnetic susceptibility, and thermodynamic calculations: Geological Society of America Bulletin, v. 121, no. 5-6, p. 919-938.
Craddock, J. P., Nielson, K. J., and Malone, D. H., 2000, Calcite twinning strain constraints on the emplacement rate and kinematic pattern of the upper plate of the Heart Mountain Detachment: Journal of Structural Geology, v. 22, no. 7, p. 983-991.
DeCelles, P. G., 2004, Late Jurassic to Eocene evolution of the Cordilleran thrust belt and foreland basin system, western USA: American Journal of Science, v. 304, no. 2, p. 105-168.
DeCelles, P. G., Gray, M. B., Ridgway, K. D., Cole, R. B., Srivastava, P., Pequera, N., and Pivnik, D. A., 1991, Kinematic History of a Foreland Uplift from Paleocene Synorogenic Conglomerate, Beartooth Range, Wyoming and Montana: Geological Society of America Bulletin, v. 103, no. 11, p. 1458-1475.
DeFrates, J., Malone, D. H., and Craddock, J. P., 2006, Anisotropy of magnetic susceptibility (AMS) analysis of basalt dikes at Cathedral Cliffs, WY: implications for Heart Mountain faulting: Journal of Structural Geology, v. 28, no. 1, p. 9-18.
Delaney, P. T., Pollard, D. D., Ziony, J. I., and McKee, E. H., 1986, Field relations between dikes and joints; emplacement processes and paleostress analysis: Journal of Geophysical Research, v. 91, no. B5, p. 4920-4938.
Dickinson, W. R., Klute, M. A., Hayes, M. J., Janecke, S. U., Lundin, E. R., McKittrick, M. A., and Olivares, M. D., 1988, Paleogeographic and Paleotectonic Setting of Laramide Sedimentary Basins in the Central Rocky-Mountain Region: Geological Society of America Bulletin, v. 100, no. 7, p. 1023-1039.
Douglas, T. A., Chamberlain, C. P., Poage, M. A., Abruzzese, M., Shultz, S., Henneberry, J., and Layer, P., 2003, Fluid flow and the Heart Mountain fault: a stable isotopic, fluid inclusion, and geochronologic study: Geofluids, v. 3, no. 1, p. 13-32.
Dunne, W. M., Ferrill, D. A., Crider, J. G., Hill, B. E., Waiting, D. J., and La Femina, P. C., 2003, Orthogonal jointing during coeval igneous degassing and normal faulting, Yucca Mountain, Nevada: Geological Society of America Bulletin, v. 115, no. 12, p. 1492-1509.
Erslev, E. A., 1993, Thrusts, back-thrusts, and detachment of Rocky Mountain foreland arches: Special Paper - Geological Society of America, v. 280, p. 339-358.
Feeley, T. C., 2003, Origin and tectonic implications of across-strike geochemical variations in the Eocene Absaroka volcanic province, United States: Journal of Geology, v. 111, no. 3, p. 329-346.
Feeley, T. C., and Cosca, M. A., 2003, Time vs. composition trends of magmatism at Sunlight volcano, Absaroka volcanic province, Wyoming: Geological Society of America Bulletin, v. 115, no. 6, p. 714-728.
Foose, R. M., Wise, D. U., and Garbarini, G. S., 1961, Structural geology of the Beartooth Mountains, Montana and Wyoming: Geological Society of America Bulletin, v. 72, no. 8, p. 1143-1172.
Gingerich, P. D., 1983, Paleocene-Eocene faunal zones and a preliminary analysis of Laramide structure deformation in the Clark's Fork Basin, Wyoming: Guidebook - Wyoming Geological Association, v. 34, p. 185-195.

Gingerich, P. D., and Clyde, W. C., 2001, Overview of mammalian biostratigraphy in the Paleocene-Eocene Fort Union and Willwood formations of the Bighorn and Clark's Fork basins, Volume Vol. 33: Papers on Paleontology, University of Michigan, Museum of Paleontology: Ann Arbor, MI, United States, p. 1-14.

Goren, L., Aharonov, E., and Anders, M. H., 2010, The long runout of the Heart Mountain landslide: Heating, pressurization, and carbonate decomposition: Journal of Geophysical Research-Solid Earth, v. 115.

Gries, R., 1983, North-South compression of Rocky Mountain foreland structures: Field Conference - Rocky Mountain Association of Geologists, v. 1983, p. 9-32.

Hacker, D. B., Biek, R. F., and Rowley, P. D., 2014, Catastrophic emplacement of the gigantic Markagunt gravity slide, southwest Utah (USA); implications for hazards associated with sector collapse of volcanic fields: Geology [Boulder], v. 42, no. 11, p. 943-946.

Hauge, T. A., 1985, Gravity-Spreading Origin of the Heart Mountain Allochthon, Northwestern Wyoming: Geological Society of America Bulletin, v. 96, no. 11, p. 1440-1456.

Hauge, T. A., 1990, Kinematic Model of a Continuous Heart Mountain Allochthon: Geological Society of America Bulletin, v. 102, no. 9, p. 1174-1188.

Hauge, T. A., 1993, The Heart Mountain detachment, northwestern Wyoming; 100 years of controversy: Memoir - Geological Survey of Wyoming, v. 5, p. 530-571.

Hewett, D. F., 1920, The Heart Mountain overthrust,. Wyoming: Journal of Geology, v. 28, no. 6, p. 536-557.

Jackson, W. T., Bartholomew, M. J., Dupre, W. R., Armstrong, T. F., and Stewart, K. G., 2016, Campanian Paleoseismites of the Elk Basin Anticline, Northern Bighorn Basin, USA: a Record of Initial Laramide Deformation: Journal of Sedimentary Research, v. 86, no. 4, p. 394-407.

Koide, H., and Bhattacharji, S., 1975, Formation of fractures around magmatic intrusions and their role in ore localization: Economic Geology and the Bulletin of the Society of Economic Geologists, v. 70, no. 4, p. 781-799.

Malone, D. H., 2000, Structure and stratigraphy of Eocene volcanic rocks in the proximal areas of the Heart Mountain Detachment: Guidebook - Wyoming Geological Association, v. 51, p. 29-50.

Malone, D. H., and Craddock, J. P., 2008a, Recent contributions to the understanding of the Heart Mountain Detachment, Wyoming: Northwest Geology, v. 37, p. 21-40.

Malone, D. H., Craddock, J. P., Anders, M. H., and Wulff, A., 2014, Constraints on the Emplacement Age of the Heart Mountain Slide, Northwestern Wyoming: Journal of Geology, v. 122, no. 6, p. 671-685.

Malone, D. H., Craddock, J. P., Schmitz, M. D., Kenderes, S., Kraushaar, B., Murphey, C. J., Nielsen, S., and Mitchell, T. M., 2017, In abstract: Volcanic Initiation of the Eocene Heart Mountain Slide, Wyoming, USA: The Journal of Geology.

Mitchell, T. M., Smith, S. A. F., Anders, M. H., Di Toro, G., Nielsen, S., Cavallo, A., and Beard, A. D., 2015, Catastrophic emplacement of giant landslides aided by thermal decomposition: Heart Mountain, Wyoming: Earth and Planetary Science Letters, v. 411, p. 199-207.

Neely, T. G., and Erslev, E. A., 2009, The interplay of fold mechanisms and basement weaknesses at the transition between Laramide basement-involved arches, north-central Wyoming, USA: Journal of Structural Geology, v. 31, no. 9, p. 1012-1027.

Neser, L. R., 2014, The Timing of Laramide Deformation in the Northern Rocky Mountains [Ph.D Dissertation: University of North Carolina at Chapel Hill, 143 p.
Petit, J. P., 1987, Criteria for the Sense of Movement on Fault Surfaces in Brittle Rocks: Journal of Structural Geology, v. 9, no. 5-6, p. 597-608.
Pierce, W. G., 1957, Heart Mountain and South Fork detachment thrusts of Wyoming: Bulletin of the American Association of Petroleum Geologists, v. 41, no. 4, p. 591-626.
Pierce, W. G., 1973, Principal Features of the Heart Mountain Fault and the Mechanism Problem: United States, John Wiley & Sons, New York, p. 457-471.
Pierce, W. G., 1975, Principal features of the Heart Mountain Fault and the mechanism problem: Guidebook - Wyoming Geological Association, no. 27, p. 139-148.
Pierce, W. G., 1987, The case for tectonic denudation by the Heart Mountain Fault; a response: Geological Society of America Bulletin, v. 99, no. 4, p. 552-568.
Pollard, D. D., and Aydin, A., 1988, Progress in Understanding Jointing Over the Past Century: Geological Society of America Bulletin, v. 100, no. 8, p. 1181-1204.
Stewart, K. G., Bartholomew, M. J., and Ballantyne, H. A., 2008, Laramide paleoseismites of the Bighorn Basin: GSA Field Guide, v. 10, p. 249-263.
Sundell, K. A., 1993, A geologic overview of the Absaroka volcanic province: Memoir - Geological Survey of Wyoming, v. 5, p. 480-506.
W. S. G. Survey, 2014, Wyoming Bedrock Geology, vector digital data, http://www.wsgs.wyo.gov/gis-files/bedrock-500k.zip, http://www.wsgs.wyo.gov/.
Swanson, E., Wernicke, B. P., and Hauge, T. A., 2016, Episodic Dissolution, Precipitation, and Slip along the Heart Mountain Detachment, Wyoming: Journal of Geology, v. 124, no. 1, p. 75-97.
Templeton, A. S., Sweeney, J., Manske, H., Tilghman, J. F., Calhoun, S. C., Violich, A., and Chamberlain, C. P., 1995, Fluids and the Heart-Mountain Fault Revisited: Geology, v. 23, no. 10, p. 929-932.
Wilkins, S. J., Gross, M. R., Wacker, M., Eyal, Y., and Engelder, T., 2001, Faulted joints; kinematics, displacement-length scaling relations and criteria for their identification: Journal of Structural Geology, v. 23, no. 2-3, p. 315-327.
Wise, D. U., 2000, Laramide structures in basement and cover of the Beartooth uplift near Red Lodge, Montana: AAPG Bulletin-American Association of Petroleum Geologists, v. 84, no. 3, p. 360-375.
Wise, D. U., and McCrory, T. A., 1982, A new method of fracture analysis; azimuth versus traverse distance plots: Geological Society of America Bulletin, v. 93, no. 9, p. 889-897.